NACA

RESEARCH MEMORANDUM

WIND-TUNNEL INVESTIGATION AT MACH NUMBERS FROM 0.50 TO 1.29 OF AN ALL-MOVABLE TRIANGULAR WING OF ASPECT RATIO 4 ALONE AND WITH A BODY

By Louis S. Stivers, Jr., and Alexander W. Malick

Ames Aeronautical Laboratory
Moffett Field, Calif.

NATIONAL ADVISORY COMMITTEE
FOR AERONAUTICS

WASHINGTON
February 2, 1950

WIND-TUNNEL INVESTIGATION AT MACH NUMBERS FROM 0.50 TO 1.29 OF AN ALL-MOVABLE TRIANGULAR WING OF ASPECT RATIO 4 ALONE AND WITH A BODY

By Louis S. Stivers, Jr., and Alexander W. Malick

SUMMARY

The aerodynamic characteristics of an all-movable, triangular-plan-form wing alone and with a body have been determined from semispan model tests. The wing had an aspect ratio of 4 and had doubly symmetrical double-wedge sections with maximum thickness-chord ratios of 0.08 in the streamwise direction. The experimental data were obtained at Mach numbers from 0.50 to about 0.98 and from 1.09 to 1.29 with corresponding Reynolds numbers varying from about 0.8×10^6 to 1.1×10^6. Calculated characteristics were compared with the corresponding experimental results.

The agreement between the calculated and experimental results was not satisfactory for the most part. The disagreement was thought to result from the failure of the linear theory to define the actual flow field about the configurations investigated, and from the effect of the tunnel-wall boundary layer on the experimental results. For the case of the wing in the presence of the body, however, it appeared that the flow about the wing was influenced very little by the tunnel-wall boundary layer.

The experimental lift-curve slopes for the wing and body, and for the wing in the presence of the body (body attitude 0°), were about 15 percent less than the corresponding calculated values at the subsonic Mach numbers up to 0.85 and at the supersonic Mach numbers. The experimental locations of the aerodynamic center for the wing alone and in the presence of the body were not predicted by the calculations, but the effect of the body on the observed aerodynamic-center location was in good agreement with that calculated.

INTRODUCTION

Low-aspect-ratio, all-movable wings or control surfaces have been proposed for highly maneuverable supersonic aircraft as a means for providing greater aircraft control at transonic and supersonic Mach numbers than that obtainable by the use of conventional control surfaces.

In such application, it is desirable that the all-movable lifting surface should exhibit throughout the entire range of flight Mach numbers very little variation in the aerodynamic-center location and an adequate amount of lift effectiveness. The former requirement is satisfied by the use of triangular-plan-form lifting surfaces of very low aspect ratio; whereas the latter may prescribe lifting surfaces of higher aspect ratio. As a consequence, it appears that a compromise would confront the designer contemplating the use of an all-movable wing or control surface on supersonic aircraft.

It is expected that the design of all-movable lifting surfaces will be dictated largely by information available from experimental investigations, yet only a small amount of such data exists. Recourse to theory does not necessarily lead to satisfactory design data. Furthermore, in the transonic Mach number range the applicability of existing theory would be generally questionable. In order to provide experimental data in the transonic Mach number range applicable to the design of triangular-plan-form, all-movable lifting surfaces, an investigation has been made of an all-movable wing in the Ames 1- by 3-1/2-foot high-speed wind tunnel. The results of this investigation are presented herein for the wing alone and with a body at Mach numbers from 0.50 to about 0.98 and from 1.09 to 1.29. In addition, calculations based on the theories of references 1 to 5 are presented for comparison with the experimental data.

NOTATION

A aspect ratio

c chord of wing measured in streamwise direction

$\bar{c}$ mean aerodynamic chord of exposed wing surface $\left(\frac{\int c^2 dy}{\int c\, dy}\right)$

C_D drag coefficient based on the exposed wing area

C_{D_L} drag coefficient due to laminar skin friction

C_{D_T} drag coefficient due to turbulent skin friction

$C_{D_{min}}$ minimum drag coefficient

$\frac{\Delta C_D}{(\Delta C_L)^2}$ drag-rise factor, average ratio of the increment of drag coefficient above the minimum to the square of the increment of lift measured from that corresponding to minimum drag coefficient $\left[\frac{C_D - C_{D_{min}}}{(C_L - C_L \text{ at } C_{D_{min}})^2}\right]_{av}$

C_L lift coefficient based on the exposed wing area

C_m pitching-moment coefficient of wing about quarter-chord point of mean aerodynamic chord based on the exposed wing area, with mean aerodynamic chord as reference length

M free-stream Mach number

R Reynolds number based on the mean aerodynamic chord of wing

R_{av} Reynolds number based on average chord of wing

y spanwise distance measured from wing root-chord line

α wing angle of attack, degrees

α' wing angle of attack, uncorrected for tunnel jet-boundary interference, degrees

DESCRIPTION OF APPARATUS

The investigation was conducted in the Ames 1- by 3-1/2-foot high-speed wind tunnel, a single-return closed-throat tunnel vented to the atmosphere in the return passage. During the investigation the tunnel was equipped with a flexible-throat assembly (fig. 1) to permit operation at various supersonic, as well as at subsonic, Mach numbers.

The test models consisted of a semispan all-movable wing and a half-body. Principal dimensions of the models are shown in figure 2. The wing model was one-half a complete wing which had a triangular plan form of aspect ratio 4. Sections in a streamwise direction were doubly symmetrical double-wedge profiles having a maximum thickness of 8 percent of the chord. The wing was rotated about a spindle axis which was perpendicular to the root chord at the 50-percent-chord point. (See fig. 2.) The spindle was fitted with an electrical resistance strain gage for measuring pitching moments of the wing. The wing was constructed of tool steel, hardened, ground, and polished; and the leading- and trailing-edge radii were approximately 0.002 inch.

The body was one-half of a 2-1/2-inch-diameter body of revolution with identical pointed ends. (See fig. 2.) The body was constructed of aluminum alloy and the surface was polished.

For the investigation, the models were mounted on a balance plate which was held in an approximately 18-inch-diameter opening in the tunnel sidewall, as shown in the photographs of figure 3. The face of the balance plate exposed to the tunnel air stream was flush with the tunnel sidewall, and an approximately 1/16-inch annular gap was maintained

between the periphery of the plate and the sidewall. A housing prevented flow through this gap from the atmosphere. The balance-plate supports were fitted with electrical resistance strain gages for measuring the lift and drag reactions. Lateral restraint was accomplished in such a manner as to virtually eliminate friction in a plane parallel to the balance-plate face.

For the tests of the wing alone, the model was supported from the rear face of the balance plate by the 0.4-inch-diameter spindle which extended through an approximately 0.6-inch-diameter hole in the plate. A 0.03-inch gap was maintained between the front face of the balance plate and the root of the wing.

For the wing and body tests, the half-body with a 0.05-inch spacer was mounted on the balance plate. The spacer kept the tips of the body, which extended beyond the periphery of the balance plate, free of the tunnel sidewalls. The wing spindle was fixed to the rear face of the balance plate, as in the wing-alone tests, and extended through the balance plate and a 0.53-inch-diameter hole in the body. A 0.03-inch gap was maintained between the body and the undeflected wing.

TESTS

Lift, drag, and pitching-moment data were obtained for the wing alone at angles of attack from approximately 0° to 10° and at Mach numbers from 0.50 to about 0.98 and from 1.09 to 1.29. Lift and pitching-moment data were also obtained at an angle of attack of about -3° in order to provide a check on the incidence and symmetry of the model. Tests were also made of the wing alone with the gap sealed. No pitching moments were measured when the gap was sealed; however, lift and drag data were obtained for angles of attack from approximately 0° to 9° at Mach numbers from 0.50 to about 0.98 and at 1.20 and 1.29.

Lift data for the wing-body combination and pitching-moment data for the wing in the presence of the body were obtained for wing angles of attack from about -3° to 10° at Mach numbers from 0.50 to about 0.98 and at 1.20 and 1.28. For the tests of the wing-body combination, the body attitude was fixed at 0°, and the gap between the wing root and body remained unsealed. The wing-induced lift on the body (body attitude 0°) was obtained for wing angles of attack from about -3° to 11° at Mach numbers from 0.50 to about 0.98 and at 1.20 and 1.28. For this condition, the models were mounted in an identical manner to that for the wing and body tests except that the wing spindle was held independently of the balance plate.

Choking conditions in the tunnel test section precluded testing of the wing alone between Mach numbers of about 0.98 and 1.09 and of the wing-body combination between Mach numbers of about 0.98 and 1.20.

Reynolds numbers, based on the mean aerodynamic chord of the wing, varied from approximately 0.8×10^6 at a Mach number of 0.50 to approximately 1.1×10^6 at a Mach number of 1.29, as shown in figure 4.

Stream-angle measurements were made at the model position at each test Mach number using a 3/16-inch-diameter probe with a hemispherical nose. The stream angle was determined by the inclination of the probe when equal pressures were indicated by symmetrically placed orifices located in the probe nose.

CORRECTIONS TO DATA

The wind-tunnel-wall corrections which were applied to the drag coefficients and angles of attack for the subsonic Mach numbers were determined by the methods of reference 6 and are indicated in reference 7 to be independent of Mach number. The corrections are:

Wing alone	Wing and body
$\Delta\alpha$ (deg) = 0.341 C_L	$\Delta\alpha$ (deg) = 0.549 C_L
ΔC_D = .0060 C_L^2	ΔC_D = .0096 C_L^2

The data at subsonic Mach numbers have been corrected for model and wake blockage by factors which were determined by the methods of reference 8 and which are given in table I for various corrected Mach numbers. Since these factors varied with the measured drag coefficient, only the upper and lower limits are given for each Mach number.

Tare corrections obtained while the models were held in the presence of the balance plate have been applied to both the sealed- and unsealed-gap data at all the test Mach numbers. These corrections were found to be practically independent of wing angle of attack. The lift coefficient tares are:

Wing alone		Wing and body	
Mach numbers	Lift tares	Mach numbers	Lift tares
0.50 to 0.80	0.006	0.50 to 0.90	0.002
.80 to .98	.007	.90 to .98	.001
1.09	.006	- - -	- - -
1.20	.005	1.20	.001
1.24	.002	- - -	- - -
1.29	-.001	1.28	.001

CONFIDENTIAL

The drag-coefficient tares for the balance plate alone and with the wing in the presence of the plate are presented in figure 5 as a function of Mach number.

The stream inclination at the model position was found, for the most part, to be negligibly small for all the test Mach numbers. As a consequence, no corrections to the angle of attack have been made for stream inclination.

Tunnel-wall boundary-layer measurements made at Mach numbers from 0.50 to 1.29 with the wind tunnel empty have indicated the existence of a stable, turbulent boundary layer of approximately 1.3-inch total thickness and 0.12-inch displacement thickness at the model position. Low induced pressures on the wing or body may have drained low-energy air from the tunnel-wall boundary layer such that the boundary layer on the rear portion of the wing would separate or be substantially thickened. The extent of such an interaction and to what degree the test data may have been affected, however, are unknown.

The effects of the possible flow of air around the wing spindle gap and through the gap between the balance plate and the tunnel wall are also unknown, but are believed to have been negligible.

RESULTS AND DISCUSSION

The basic results are presented as lift, drag, and pitching-moment coefficients in figures 6 to 9 as functions of Mach number for various wing angles of attack. (Mechanical difficulties with the apparatus for setting wing angles of attack resulted in fractional angles for some of the data of these figures.)

Lift Characteristics

Lift coefficient as a function of Mach number for various wing angles of attack is shown in figures 6 and 7. The lift coefficients of figure 6 are for the wing alone, with the gap at the wing root unsealed and sealed. Those for the wing and body and the body in the presence of the wing are shown in figure 7. The lift coefficients for the body, indicated in this figure, are solely those induced by the wing, since the attitude of the body was 0° throughout the tests. The variations of lift coefficient with Mach number for given angles of attack, exhibited in figures 6 and 7, are generally small. Shown in figure 10 are faired curves of the same lift coefficients plotted as a function of angle of attack at various Mach numbers from 0.50 to 1.29. The variation of lift coefficient with angle of attack is generally linear throughout the angle-of-attack range at both subsonic and supersonic Mach numbers. The

shift of the lift curves in the positive lift direction exhibited in figures 6(b) and 10(c) at subsonic Mach numbers was apparently due to a constant error in setting the incidences of the model.

The variations with Mach number of the lift-curve slopes for the wing alone, gap unsealed and sealed, are presented in figure 11(a). It is observed in this figure that the lift-curve slope for the wing with the gap unsealed varies only a small amount over the range of Mach numbers from 0.50 to 1.29. Sealing the gap increased the slope significantly at the subsonic Mach numbers and only slightly at the supersonic Mach numbers.

Calculated lift-curve slopes for the wing alone are also shown in figure 11(a). The values at subsonic Mach numbers were determined by the methods of reference 1 and those at supersonic Mach numbers by the methods of reference 2. It is apparent from this figure that the experimental lift-curve slope is much less than the calculated. As the Mach number is increased from 0.50 to 0.975, the experimental slope for the wing, gap sealed, ranges from about 9 to 28 percent less than the calculated slope. At Mach numbers of 1.20 and 1.29, the slopes corresponding to the sealed gap are, respectively, about 33 and 30 percent less than those calculated.

It is felt that the difference in the experimental and calculated lift-curve slopes for the wing is largely attributable to the effects of the following, which are not taken into account in the linear theory: (1) Interaction between the flow over the wing and that in the tunnel-wall boundary layer; (2) shock-wave boundary-layer interaction at the high subsonic and supersonic Mach numbers (discussed in references 9 and 10 for two-dimensional airfoil sections at subsonic and supersonic Mach numbers, respectively); and (3) shock waves resulting from second-order compressibility effects at the supersonic Mach numbers (discussed in reference 11 for triangular wings).

The effect of model support on the lift-curve slope at a Mach number of 1.5 may be estimated by comparing the experimental slope for a complete wing shown in figure 11(a) with an extrapolated value of the gap-sealed data for the wing of the present investigation. The experimental slope for a Mach number of 1.5 is from unpublished data obtained from tests in the Ames 1- by 3-foot supersonic wind tunnel of a triangular-plan-form complete wing (with no body) which was sting-supported from the rear. The aspect ratio, thickness-chord ratio, and section profile of this wing were identical to those of the wing of this report. It appears from figure 11(a) that an extrapolated value of the gap-sealed lift-curve slope at a Mach number of 1.5 would be less than that for the complete wing. A lower slope would be expected for the semispan wing because of the effects of the tunnel-wall boundary layer at the wing root. The experimental slope for the complete wing is about 11 percent less than that calculated. It should not be inferred, however, that the magnitude of this disagreement between the calculated

and experimental lift-curve slopes is representative for complete wings of triangular plan form at supersonic Mach numbers, since differences as high as 30 percent have been shown in the data of reference 11. Such differences for complete wings are believed to be due largely to viscous and second-order compressibility effects.

The lift-curve slopes determined from the tests of the wing and body (gap unsealed, body attitude 0°) are presented in figure 11(b). The slopes shown in this figure correspond to (1) the total lift on the wing and body, (2) the wing-induced lift on the body, and (3) the lift of the wing in the presence of the body. The slope for the latter is the difference in the slopes of the first two. It can be seen that the effect of Mach number on the lift-curve slope of the body is small; whereas for the wing and body there is an appreciable effect at the high subsonic Mach numbers. Also shown in figure 11(b) are calculated lift-curve slopes for the same three cases. Insofar as known, there are no existing theories which are directly applicable to the wing and body configuration of this report; therefore, the following procedures were employed in the calculation of the slopes.

For the calculations at subsonic Mach numbers, it was assumed that the body could be replaced by a flat surface with boundaries that are formed by extending the leading and trailing edges of the all-movable wing to the axis of symmetry of the body. The surface replacing the body remains at zero angle of attack and the all-movable wing is thought of as a flat, full-chord, partial-span, outboard control surface. The theory of reference 4 then provides a method for determining the total lift on the control surface and the fixed surface, and the distribution of lift between the two. Lift-curve slopes (rate of change of lift coefficient with control-surface deflection) calculated by the methods of this reference, however, are not specifically applicable to the present configuration since the theory is valid only for lifting surfaces of very low aspect ratio. It was believed, nevertheless, that this restriction could be alleviated, at least for a configuration of aspect ratio 4, if ratios of lift-curve slopes were employed, that is, the ratios of the slopes given by the theory of reference 4 to the slope for a wing alone of comparable plan form having very low aspect ratio (wing-alone slope, $\pi A/2$). The calculated lift-curve slopes shown in figure 11(b) at subsonic Mach numbers were then determined as the products of these ratios and the lift-curve slopes for the wing alone determined from reference 1. (See fig. 11(a).) The calculated ratios, for slopes based on the area of the movable surface, are:

1.	Total lift	1.17
2.	Lift induced on fixed surface	.24
3.	Lift on control surface in presence of fixed surface	.93

Lift-curve-slope calculations for the wing and body at supersonic Mach numbers were made by assuming that the body could again be replaced by a fixed surface. The plan form of this fixed surface can be arbitrary outside the Mach cone from the apex of the movable surface, but within the cone it is determined by extending the trailing edge of the movable surface to the axis of symmetry of the body. It was also assumed that no Mach lines crossed those from the apex of the movable surface. The lift-curve slopes were then determined from the methods of reference 5. The following expressions, for subsonic leading edges, were used to determine the slopes (based on the area of the movable surface) shown in figure 11(b) at the supersonic Mach numbers:

1. Total lift

$$\frac{C_L}{\alpha} = \frac{4}{\sqrt{M^2-1}} k^{1/2}$$

2. Lift induced on fixed surface

$$\frac{C_L}{\alpha} = \frac{8}{\sqrt{M^2-1}} \frac{k^{1/2}}{\pi(1+k)} \left[\frac{\pi(1+k)}{2} - k^{1/2} - (1+k) \tan^{-1} k^{1/2} \right]$$

3. Lift on control surface in presence of fixed surface

$$\frac{C_L}{\alpha} = \frac{8}{\sqrt{M^2-1}} \frac{k^{1/2}}{\pi(1+k)} \left[k^{1/2} + (1+k) \tan^{-1} k^{1/2} \right]$$

where k is $\cot \Lambda \sqrt{M^2-1}$ and Λ is the leading-edge sweep angle of the movable surface (positive for sweepback).

It is observed in figure 11(b) at both the subsonic and supersonic Mach numbers that the experimental lift-curve slopes are less than those calculated, but the agreement between the two is much better than that for the wing alone. For Mach numbers up to 0.85, the experimental lift-curve slopes for the wing and body (wing lift plus induced lift on body) are about 14 percent less than those calculated; whereas those for the wing in the presence of the body are about 17 percent less. The experimental and calculated slopes for the induced lift on the body are in good agreement at all the subsonic Mach numbers. At supersonic Mach numbers the experimental slopes for the wing and body are about 16 percent less than those calculated; those for the wing in the presence of the body, about 13 percent less; and those for the induced lift on the body, from about 25 to 30 percent less. These disagreements between the calculated and experimental slopes are considered to be generally small in view of the procedure and theory employed, and of the neglect, in common with the theory for the wing alone, of viscous and second-order compressibility effects. Because the agreement between the calculated and

experimental lift-curve slopes is generally so much better for the wing in the presence of the body than for the wing alone, it is felt that the influence of the tunnel-wall boundary layer on the flow around the wing in the presence of the body was small. Although there may have been a significant effect of the tunnel-wall boundary layer on the lift induced on the body, such an effect appears to have influenced the combined lifts of the wing and body but very little. This is undoubtedly due to the fact that the body lift is only a small part of the total.

It is of interest to note the difference between the calculated and experimental lift-curve slopes for a semispan all-movable triangular wing tested in the presence of a body at a Mach number of 1.9 and reported in reference 12. The wing of this reference had an aspect ratio of 2.31 and circular-arc sections 9-percent chord thick, and was tested in the presence of a half-body for which the boundary layer was known to be substantially identical to that on the complete body held in the center of the wind tunnel. The lift-curve slope of this wing in the presence of the body was about 14 percent less than the corresponding slope calculated by the procedure of the present report using the theory of reference 5.

It is also of interest to note the agreement between experiment and theory in the case of a configuration for which the theory of reference 5 is more directly applicable. The results of an investigation at a Mach number of 1.9 of such a configuration (triangular wing with all-movable tip control surface) are reported in reference 13. The agreement in this case was about the same as that of the present report at supersonic Mach numbers.

The variation with Mach number of the lift-curve slopes for the wing alone and for the wing in the presence of the body is compared in figure 11(c). Although the effect of Mach number on the lift-curve slope is slightly different for the two configurations, the slopes at a given Mach number differ by an amount never greater than about 10 percent. This comparison, however, may not be of particular significance in view of the probable differences in the effects of the tunnel-wall boundary layer in the two cases. From the calculations shown in figures 11(a) and 11(b), which do not account for the gap, it would be expected that the lift-curve slope for the wing in the presence of the body would be about 7 percent less than that for the wing alone at subsonic Mach numbers, and about 20 to 25 percent less at the supersonic Mach numbers.

Drag Characteristics

Drag coefficient as a function of Mach number for the wing alone, gap unsealed, is shown in figure 8 for various angles of attack. The drag coefficients for the wing with the gap sealed are not presented since they are essentially the same as those for the wing with the gap

unsealed. It is indicated in this figure that substantial changes in the rate of increase of the drag coefficients can be expected between Mach numbers of 0.975 and 1.09. Faired curves of drag coefficient as a function of lift coefficient (gap unsealed) are given in figure 12 for various Mach numbers from 0.50 to 1.29. Minimum drag coefficients determined from this figure are shown in figure 13 as a function of Mach number. Also shown in this figure for both subsonic and supersonic Mach numbers are calculated drag coefficients which correspond to either laminar or turbulent skin friction over the entire upper and lower wing surfaces. These calculations were made using the laminar and turbulent skin-friction equations of reference 14 and a Reynolds number based on the average chord of the wing. The drag-coefficient equations for both surfaces of the wing are:

$$C_{D_L} = 2.656\ R_{av}^{-1/2} \quad \text{(laminar)}$$

and

$$C_{D_T} = 0.910\ (\log_{10} R_{av})^{-2.58} \quad \text{(turbulent)}$$

The calculated drag coefficients shown at supersonic Mach numbers are the sums of the calculated skin-friction and pressure drag coefficients. The pressure drag coefficients were determined by the methods of reference 2 for a complete triangular wing of aspect ratio, thickness-chord ratio, and profile identical to those of the wing of this report.

It can be observed in figure 13 that the experimental minimum drag coefficient at low subsonic Mach numbers is in reasonable agreement with the calculated values. At Mach numbers between 0.80 and 0.975, the large increase in the experimental drag coefficients above the calculated drag coefficients corresponding to turbulent skin friction is believed to have resulted from a thickening or a separation of the boundary layer on the rear portion of the wing.

At supersonic Mach numbers, the experimental minimum drag coefficients of figure 13 are much less than the values shown for the sum of the pressure drag and the laminar or turbulent skin-friction coefficients, and are even less than the calculated pressure drag coefficients. The pressures on the upper surface of the wing near the trailing edge were apparently higher than those calculated (resulting in a reduced pressure drag), probably because of the effects of shock-wave boundary-layer interaction and of the tunnel-wall boundary layer at the wing root. The extent to which the pressures on the aft portion of a two-dimensional airfoil section may be influenced by shock-wave boundary-layer interaction at supersonic Mach numbers is shown in reference 10.

It can be seen in figure 13 for a Mach number of 1.5 that the minimum drag coefficient of a complete wing, tested in a flow field which

was apparently unaffected by the tunnel-wall boundary layer, is also lower than would be predicted. (This value of experimental minimum drag coefficient is from the unpublished test data of the complete wing described earlier in the discussion of the lift-curve slopes.) It is observed that the experimental minimum drag coefficient for the complete wing is equivalent to the calculated pressure drag coefficient which does not include skin friction.

Disagreements between the calculated and experimental minimum drag coefficients at supersonic Mach numbers similar to those noted in figure 13 are shown in reference 11 for several complete wings of triangular plan form. Such disagreements for complete wings are believed to result from the effects of shock-wave wing-boundary-layer interaction.

The variation of the experimental drag-rise factor $\Delta C_D/(\Delta C_L)^2$ with Mach number is presented in figure 14 for the wing alone, gap unsealed and sealed. Reciprocals of the experimental lift-curve slopes, gap unsealed and sealed, are also shown in figure 14 at both subsonic and supersonic Mach numbers. These reciprocals may be regarded as upper boundaries of the drag-rise factors and they indicate that the resultant force vectors are substantially perpendicular to the chord line of the wing. They do not necessarily correspond to zero leading-edge thrust, however, because of separation and friction effects. In addition to the reciprocals of the slopes, a calculated lower boundary of the drag-rise factor corresponding to full theoretical leading-edge thrust on a triangular-plan-form wing of aspect ratio 4 is shown in figure 14 at subsonic and supersonic Mach numbers. For this lower boundary, the resultant force vector is inclined at its maximum calculated forward position with respect to the wing-chord line. The subsonic values of this calculated drag-rise factor were determined by the methods of reference 1, but for all practical purposes are equivalent to the constant $1/\pi A$. The values at supersonic Mach numbers were determined by the methods of reference 3.

In figure 14, it is observed that the experimental curves for the drag-rise factor of the wing, gap unsealed, generally lie much closer to the upper drag-rise-factor boundary than to the lower. This would indicate that the drag due to lift is, for the most part, relatively high (i.e., the resultant force vector is nearly perpendicular to the chord plane of the wing). The effect of sealing the gap was, in general, to reduce appreciably the drag-rise factor at subsonic Mach numbers. At the supersonic Mach numbers the reduction was negligible.

Pitching-Moment Characteristics

The pitching-moment coefficients for the wing both alone and in the presence of the body, gap unsealed, are presented in figure 9 as a function of Mach number for various wing angles of attack. Small variations of

pitching-moment coefficients with Mach number for given angles of attack at both subsonic and supersonic Mach numbers are shown, except for angles of 6° or greater at high subsonic Mach numbers and at Mach numbers near 1.09. The pitching-moment coefficients shown in figure 9 are plotted as a function of angle of attack at constant Mach numbers in figure 15. The curves of this figure for the wing both alone and in the presence of the body are generally nonlinear at the subsonic Mach numbers, but are nearly straight at the supersonic Mach numbers. It can also be observed that at subsonic Mach numbers the effect of the body on the pitching-moment coefficients of the wing was small at low angles of attack, but a sizable destabilizing effect occurred at the high angles of attack. At supersonic Mach numbers the effect of the body was generally small.

The slopes of the pitching-moment curves $dC_m/d\alpha$ at zero angle of attack are given in figure 16. It can be seen in this figure that the slopes for the wing alone and for the wing in the presence of the body are substantially identical throughout the range of test Mach numbers.

The effects of Mach number on the location of the aerodynamic center at zero angle of attack for the wing both alone and in the presence of the body, gap unsealed, are shown in figure 17. The calculated location for the wing alone, determined from references 1 and 2, is also shown in this figure at subsonic and supersonic Mach numbers. Calculations for the wing in the presence of the body indicate that the aerodynamic-center location at the subsonic Mach numbers is about 1 percent of the mean aerodynamic chord behind that calculated for the wing alone; whereas at supersonic Mach numbers it is identical to that calculated for the wing alone. The differences in the experimental locations for the wing alone and for the wing in the presence of the body are practically the same as the previously mentioned calculated differences, although the experimental and calculated locations themselves are not in good agreement. Over the range of subsonic Mach numbers, the experimental location of the aerodynamic center for the wing both alone and in the presence of the body varies from about the 34- to the 39-percent point of the mean aerodynamic chord. The experimental location varies from about 1 to 5 percent of the mean aerodynamic chord behind the calculated location. At supersonic Mach numbers, the location of the aerodynamic center for the wing both alone and in the presence of the body, shown in figure 17, is practically a constant at about 45 percent of the mean aerodynamic chord. It is observed that the experimental location of the aerodynamic center is approximately 5 percent of the mean aerodynamic chord forward of the calculated location. An experimental location of the aerodynamic center approximately 5 percent forward of the calculated location for the wing alone is also observed from the data of reference 12, which were obtained from an investigation of a triangular all-movable wing (gap unsealed) tested in the presence of a body at a Mach number of 1.9.

An over-all rearward shift of the aerodynamic-center location of about 11 percent of the mean aerodynamic chord is shown in figure 17 for the subsonic and supersonic Mach numbers. It is of interest to note that experimental data of references 15 and 16 for complete triangular wings of aspect ratio 2 show about a 10-percent over-all shift in the aerodynamic-center location for the same ranges of Mach number.

CONCLUDING REMARKS

The calculated values of the principal aerodynamic characteristics of the all-movable triangular wing of aspect ratio 4 alone and with the body were not in good agreement, on the whole, with the corresponding experimental results. The disagreements are believed to be due to the inadequacies of the linear theories employed in describing the actual flow field about the configurations investigated and to the effects of the tunnel-wall boundary layer on the experimental results. It was noted, however, that the experimental lift-curve slopes for the wing in the presence of the body appeared to be influenced very little by the tunnel-wall boundary layer.

The experimental lift-curve slopes for the wing and body, and for the wing in the presence of the body (body attitude 0°), were about 15 percent lower than the corresponding calculated values at the subsonic Mach numbers up to 0.85 and at the supersonic Mach numbers. The experimental aerodynamic-center locations for the wing alone and in the presence of the body were not satisfactorily predicted by the calculations, but the effect of the body on the observed aerodynamic-center location was substantially the same as that calculated.

Ames Aeronautical Laboratory,
National Advisory Committee for Aeronautics,
Moffett Field, Calif.

REFERENCES

1. DeYoung, John: Theoretical Additional Span Loading Characteristics of Wings with Arbitrary Sweep, Aspect Ratio, and Taper Ratio. NACA TN 1491, 1947.

2. Puckett, A. E., and Stewart, H. J.: Aerodynamic Performance of Delta Wings at Supersonic Speeds. Jour. Aero. Sci., vol. 14, no. 10, Oct. 1947, pp. 567-578.

3. Jones, Robert T.: Estimated Lift-Drag Ratios at Supersonic Speed. NACA TN 1350, 1947.

4. DeYoung, John: Spanwise Loading for Wings and Control Surfaces of Low Aspect Ratio. NACA TN 2011, 1949.

5. Lagerstrom, P. A., and Graham, Martha E.: Linearized Theory of Supersonic Control Surfaces. Jour. Aero. Sci., vol. 16, no. 1, Jan. 1949, pp. 31-34.

6. Glauert, H.: Wind-Tunnel Interference on Wings, Bodies, and Airscrews. R. & M. No. 1566, British A.R.C., 1933.

7. Goldstein, S., and Young, A. D.: The Linear Perturbation Theory of Compressible Flow With Applications to Wind-Tunnel Interference. R. & M. No. 1909, British A.R.C., 1943.

8. Herriot, John G.: Blockage Corrections for Three-Dimensional-Flow Closed-Throat Wind Tunnels, With Consideration of the Effect of Compressibility. NACA RM A7B28, 1947.

9. Allen, H. Julian, Heaslet, Max. A., and Nitzberg, Gerald E.: The Interaction of Boundary Layer and Compression Shock and Its Effect Upon Airfoil Pressure Distributions. NACA RM A7A02, 1947.

10. Ferri, Antonio: Experimental Results With Airfoils Tested In the High-Speed Tunnel at Guidonia. NACA TM 946, 1940.

11. Love, Eugene S.: Investigation at Supersonic Speeds of 22 Triangular Wings Representing Two Airfoil Sections for Each of 11 Apex Angles. NACA RM L9D07, 1949.

12. Conner, D. William: Aerodynamic Characteristics of Two All-Movable Wings Tested in the Presence of a Fuselage at a Mach number of 1.9. NACA RM L8H04, 1948.

13. Conner, D. William, and May, Ellery B., Jr.,: Control Effectiveness Load and Hinge-Moment Characteristics of a Tip Control Surface on a Delta Wing at a Mach Number of 1.9. NACA RM L9H05, 1949.

14. von Kármán, Th.: Turbulence and Skin Friction. Jour. Aero. Sci., vol. 1, no. 1, Jan. 1934, pp. 1-20.

15. Berggren, Robert E., and Summers, James L.: Aerodynamic Characteristics at Subsonic and Supersonic Mach Numbers of a Thin Triangular Wing of Aspect Ratio 2. I- Maximum Thickness at 20 Percent of the Chord. NACA RM A8I16, 1948.

16. Walker, Harold J., and Berggren, Robert E.: Aerodynamic Characteristics at Subsonic and Supersonic Mach Numbers of a Thin Triangular Wing of Aspect Ratio 2. II- Maximum Thickness at Midchord. NACA RM A8I20, 1948.

TABLE I.- MAGNITUDE OF BLOCKAGE CORRECTIONS
[Uncorrected values multiplied by the following factors]

M	Dynamic pressure	Drag coefficient	Mach number
Wing alone			
0.50	1.000	1.000 to 0.999	1.000 to 1.001
.70	1.000 to 1.002	.999 to .998	1.000 to 1.001
.80	1.001 to 1.003	.999 to .997	1.001 to 1.003
.90	1.001 to 1.006	.998 to .994	1.001 to 1.006
.95	1.003 to 1.012	.997 to .987	1.002 to 1.012
.98	1.006 to 1.023	.995 to .972	1.008 to 1.024
Wing and body			
.50	1.008 to 1.012	.991 to .988	1.005 to 1.008
.70	1.013 to 1.018	.987 to .982	1.010 to 1.012
.80	1.020 to 1.026	.981 to .968	1.017 to 1.022
.90	1.030 to 1.040	.972 to .953	1.028 to 1.037
.95	1.040 to 1.055	.961 to .938	1.039 to 1.052
.98	1.050 to 1.072	.950 to .929	1.049 to 1.072

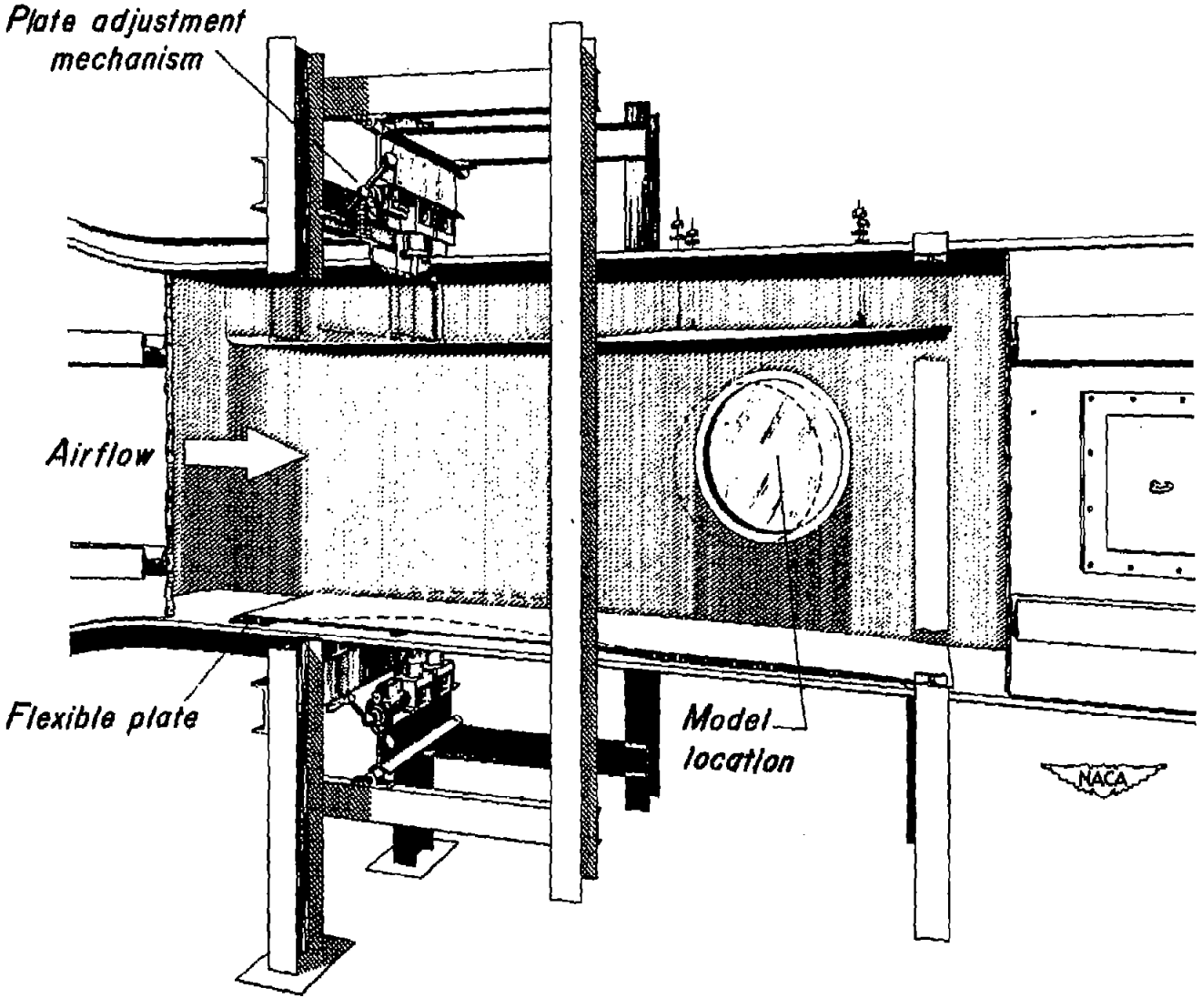

Figure 1.- Illustration of flexible-throat mechanism in the Ames 1- by 3-1/2-foot high-speed wind tunnel.

All dimensions in inches

Body coordinates	
Station	Radius
0.00	0.000
1.25	.305
2.50	.575
3.75	.790
5.00	.980
6.25	1.130
7.50	1.220
9.75	1.250
20.25	1.250
22.50	1.220
23.75	1.130
25.00	.980
26.25	.790
27.50	.575
28.75	.305
30.00	.000

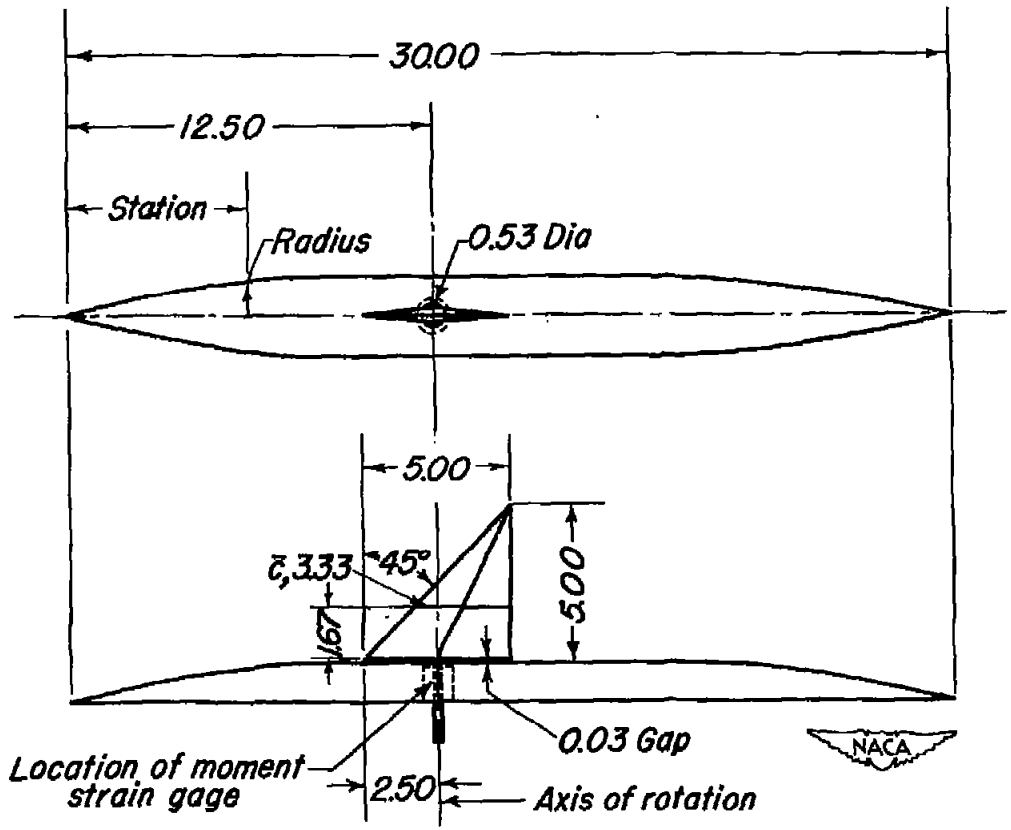

Figure 2.- Sketch of all-movable triangular wing and body.

(a) Wing alone.

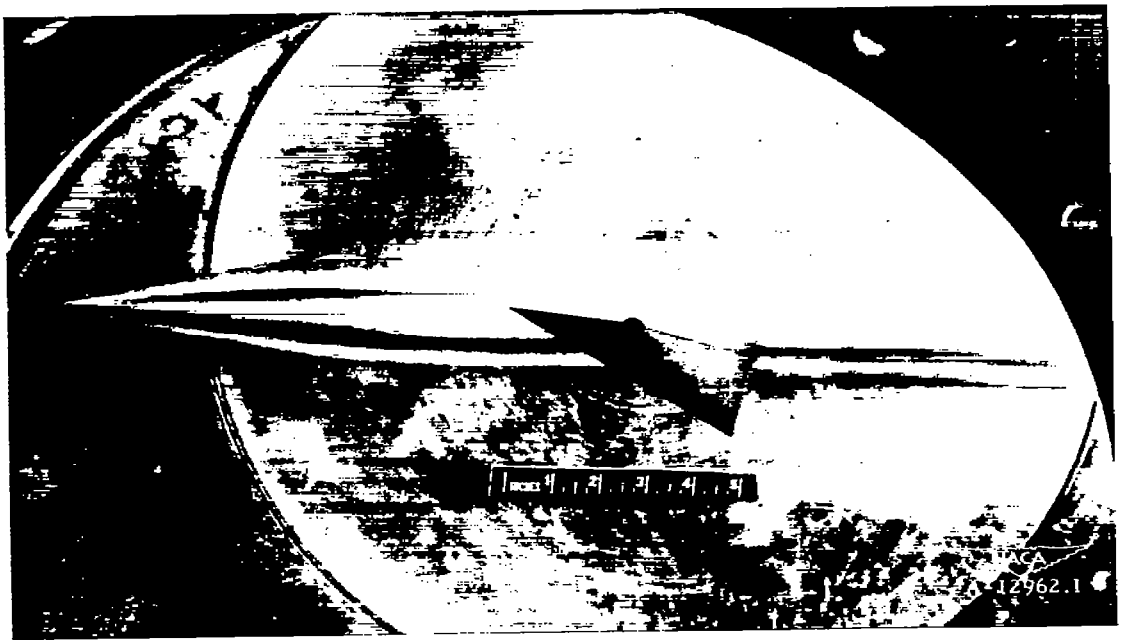

(b) Wing and body.

Figure 3.- Photographs of the all-movable triangular wing and body mounted on the balance plate in the Ames 1- by 3-1/2-foot high-speed wind tunnel.

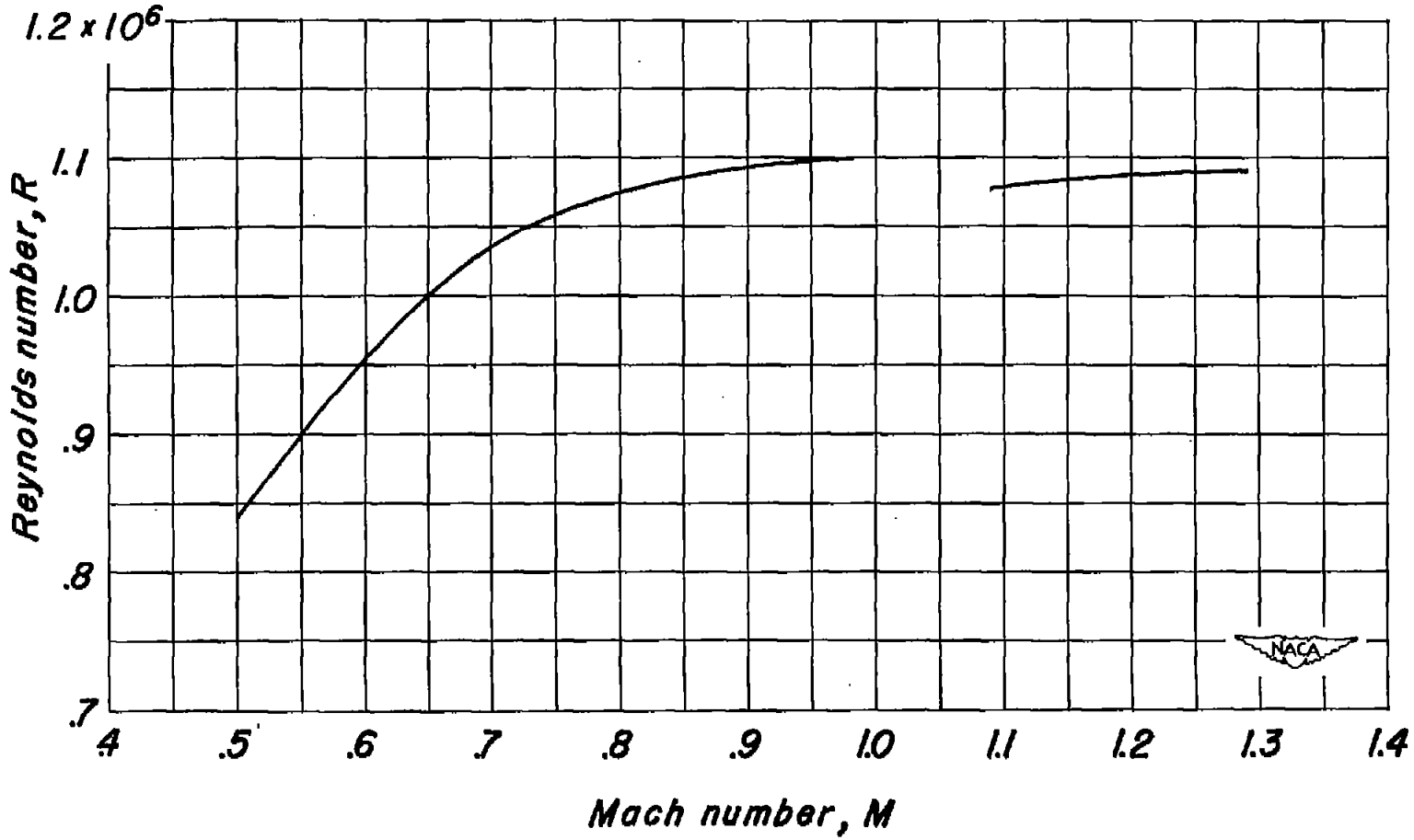

Figure 4.- The variation of Reynolds number with Mach number for the tests of the all-movable triangular wing in the Ames 1-by 3½-foot high-speed wind tunnel.

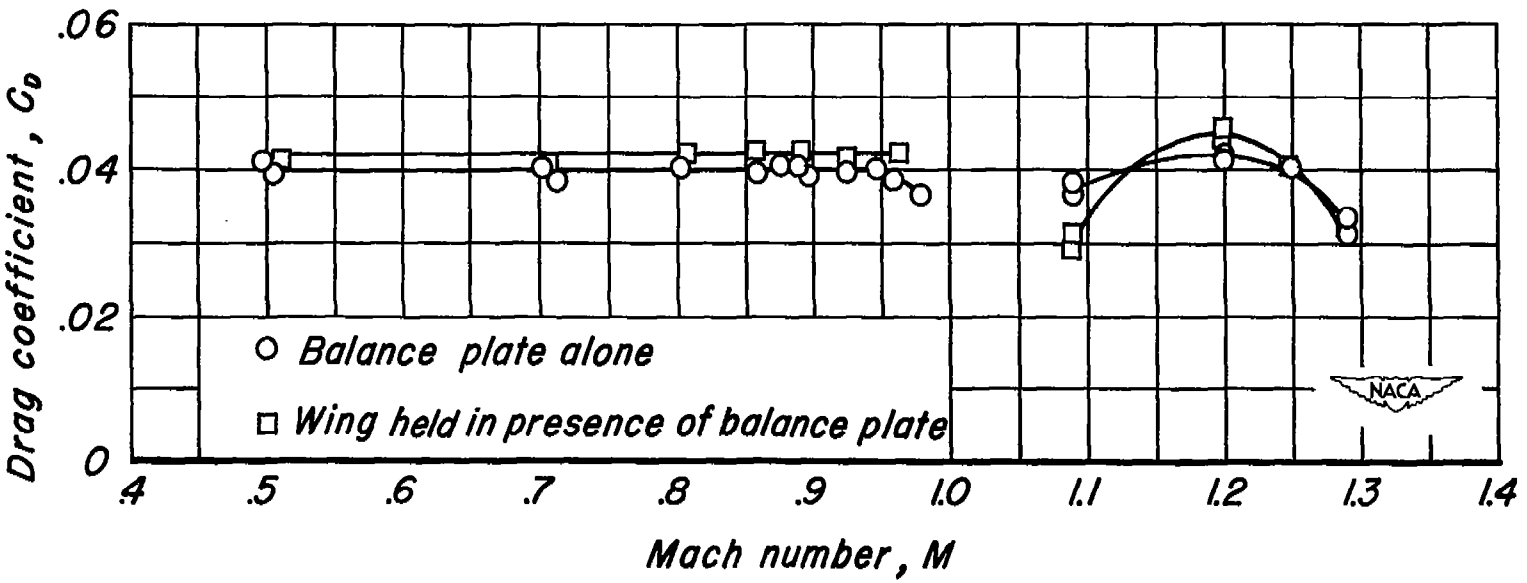

Figure 5.- Effect of Mach number on the tare drag coefficients.

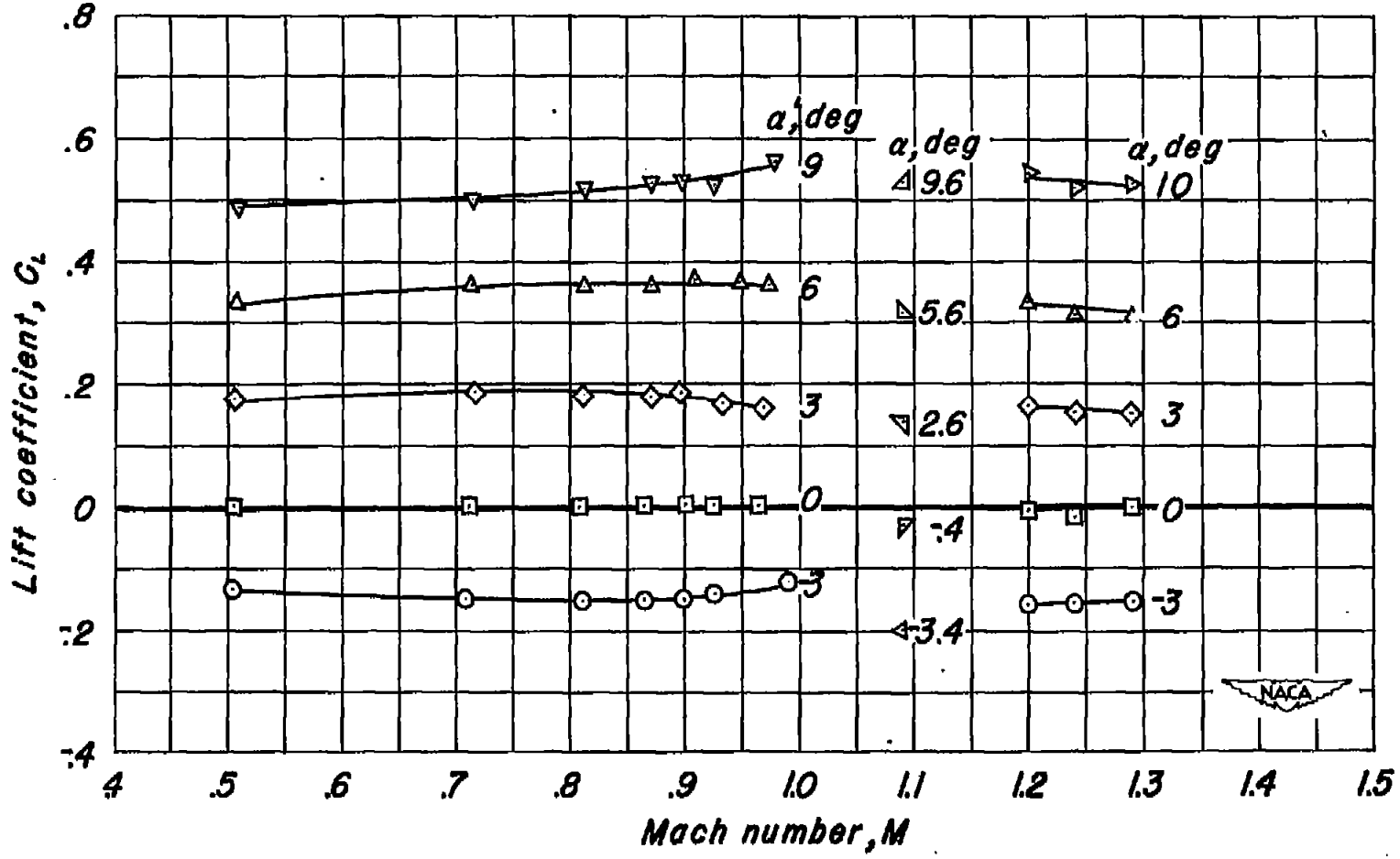

(a) Gap unsealed.

Figure 6.- Effect of Mach number on the lift coefficient of the wing alone for various angles of attack.

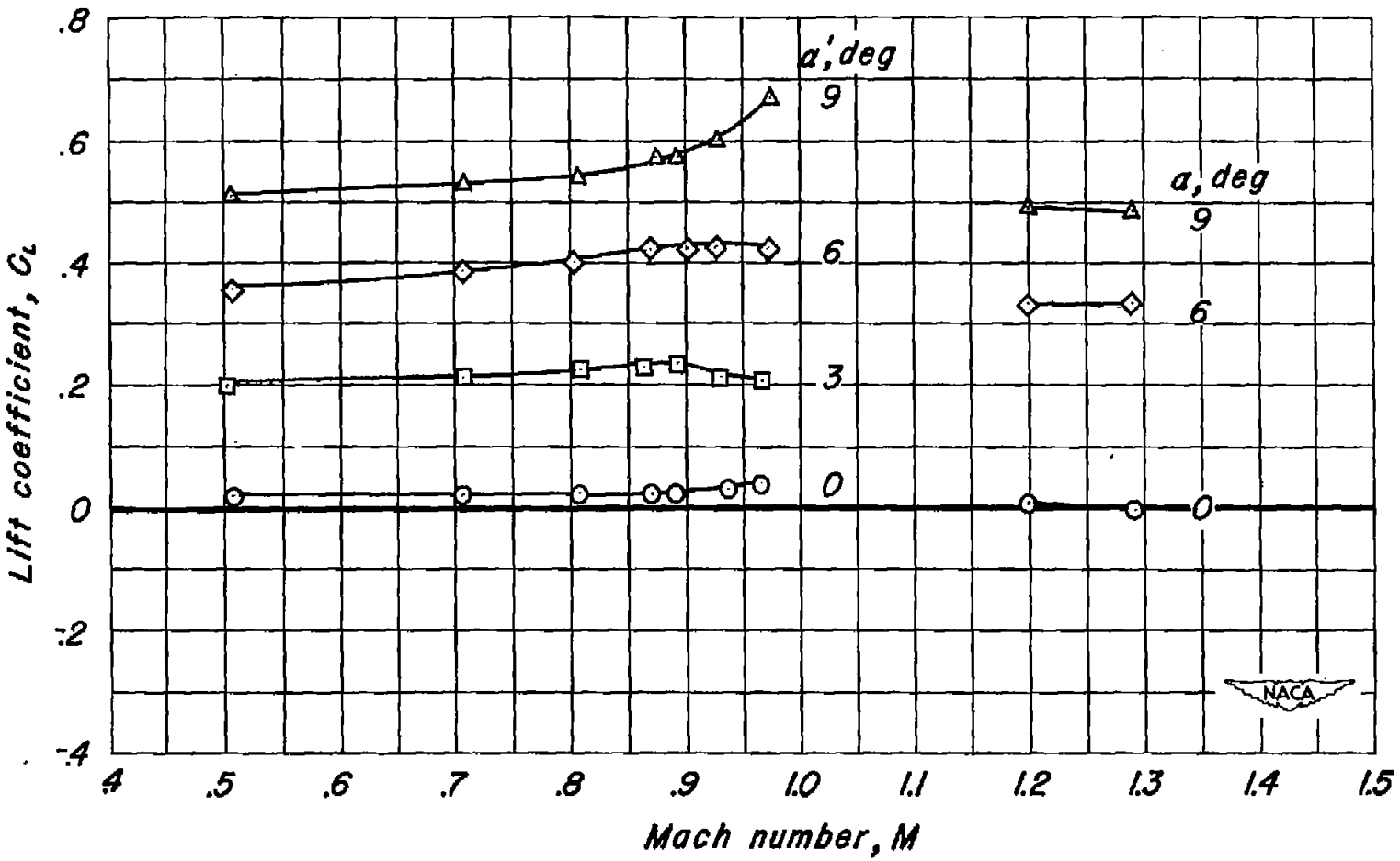

(b) Gap sealed.

Figure 6.- Concluded.

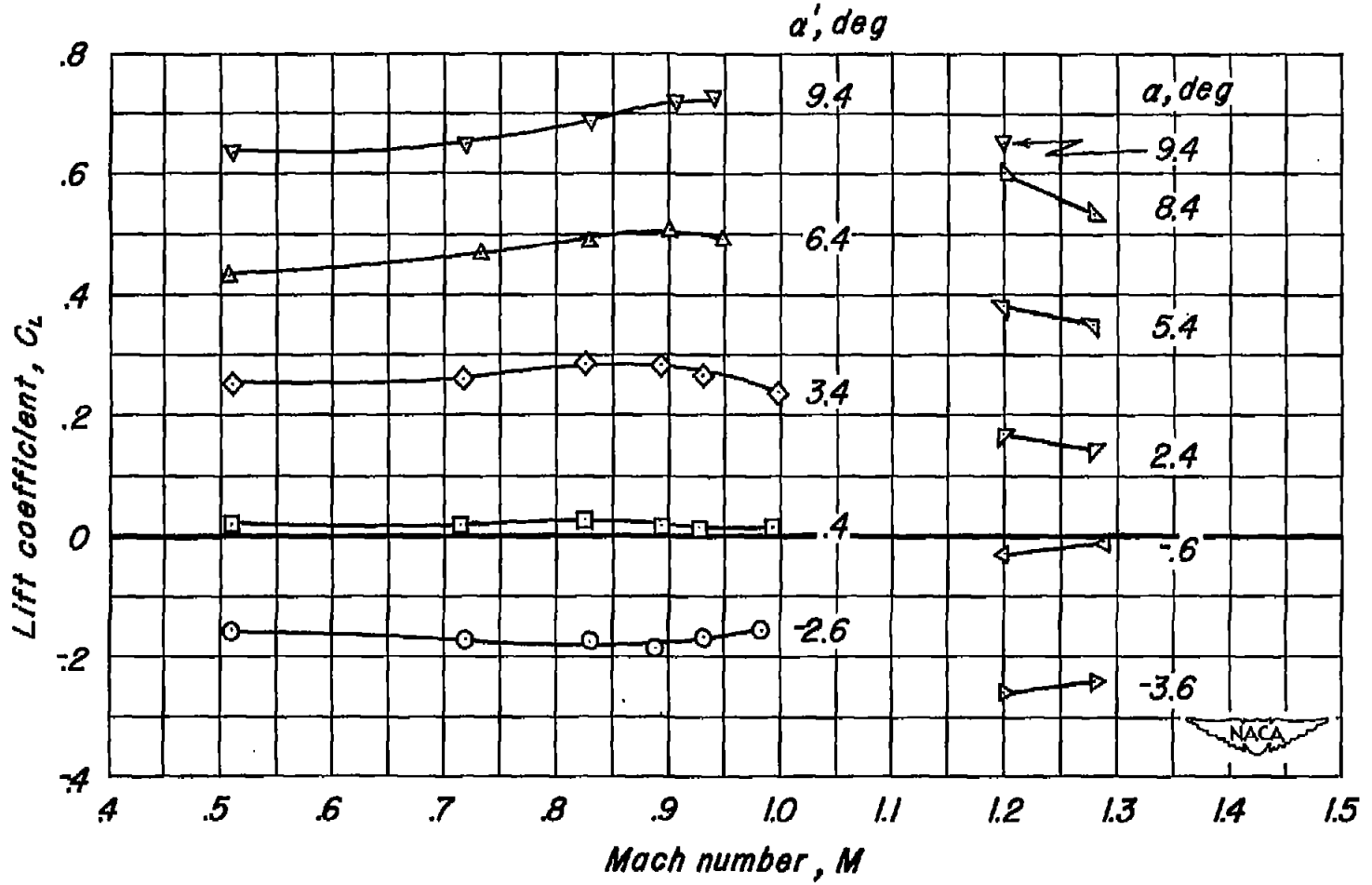

(a) Wing and body, gap unsealed.

Figure 7.- Effect of Mach number on the lift coefficient of the wing and body for various wing angles of attack. Body attitude 0°.

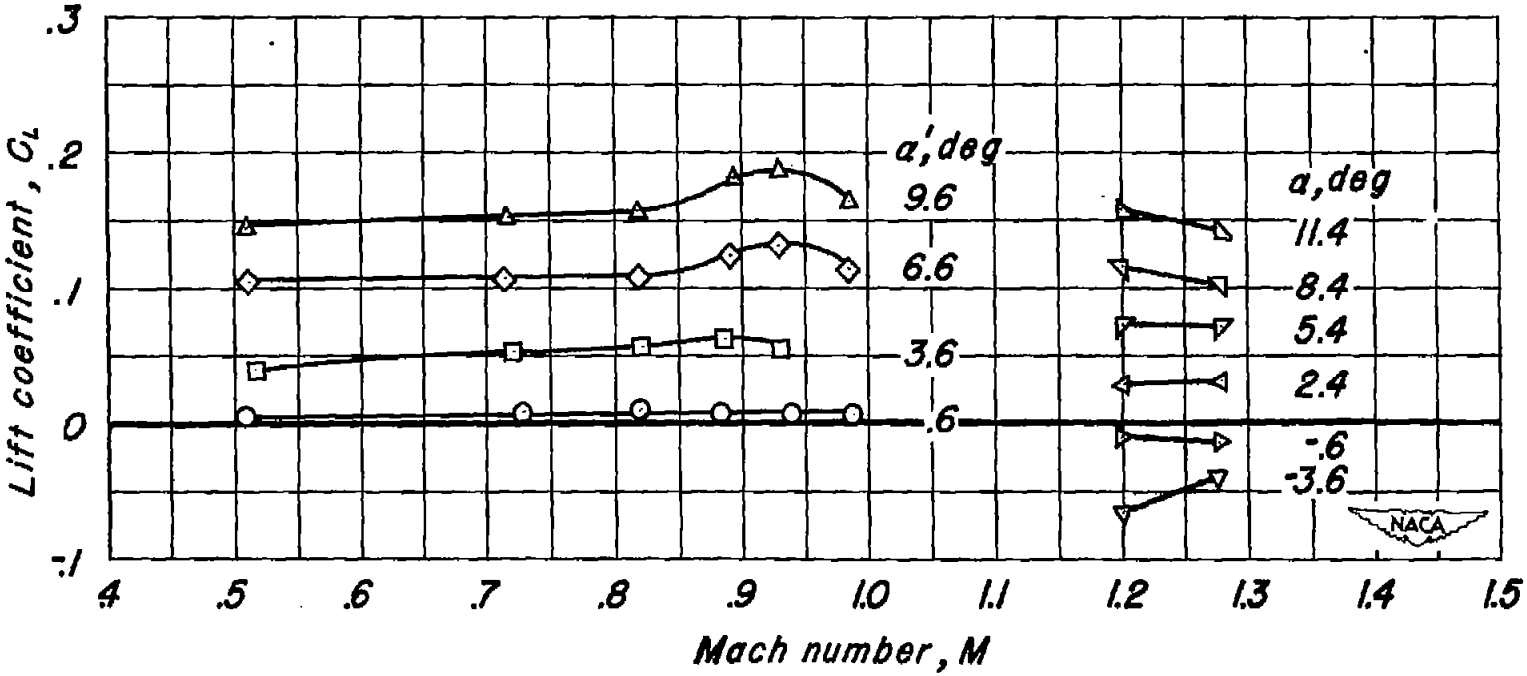

(b) Wing-induced lift on body.

Figure 7.- Concluded.

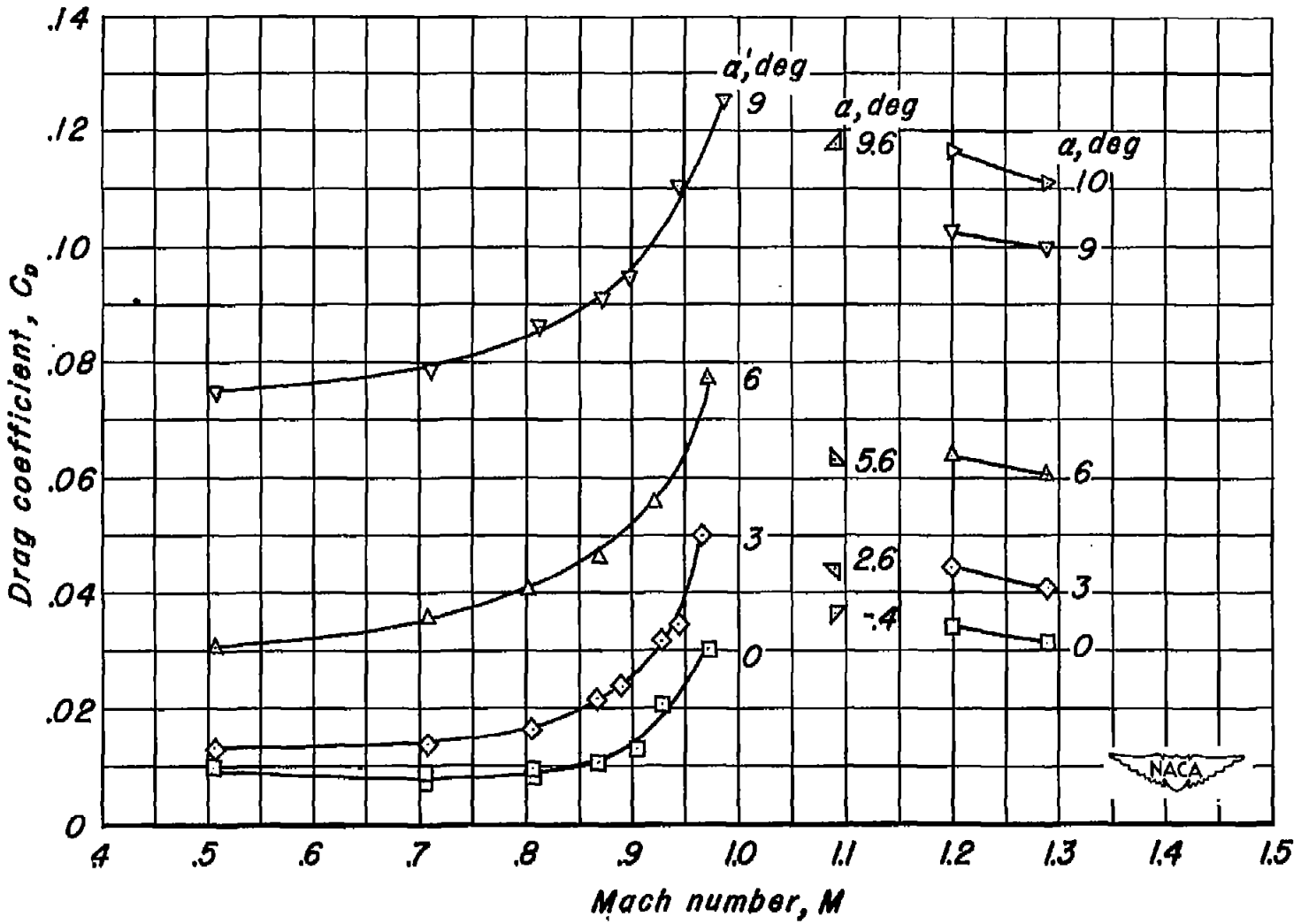

Figure 8.- Effect of Mach number on the drag coefficient of the wing alone at various angles of attack, gap unsealed.

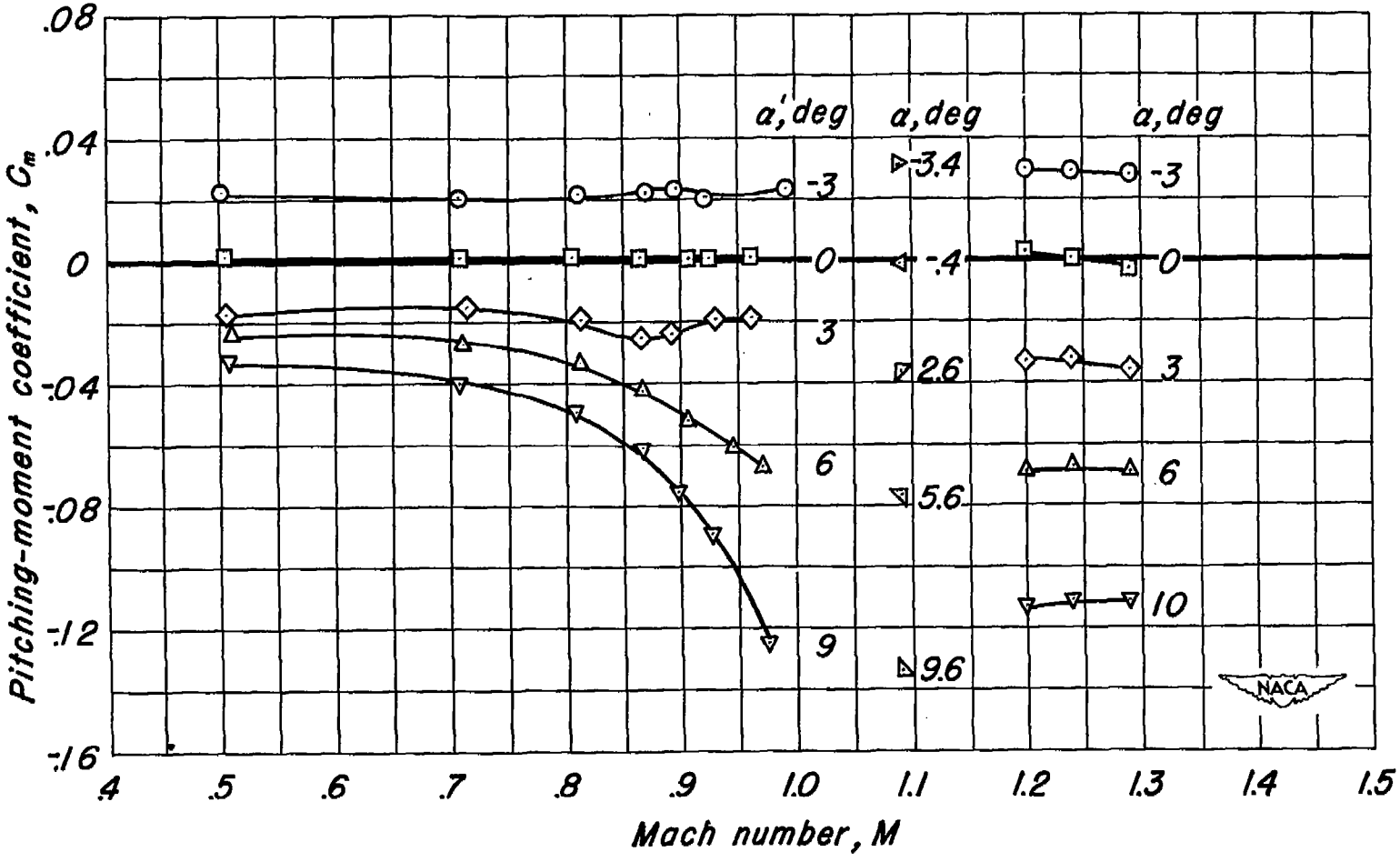

(a) Wing alone.

Figure 9.- Effect of Mach number on the pitching-moment coefficients of the wing both alone and in the presence of the body. Body attitude 0°, gap unsealed.

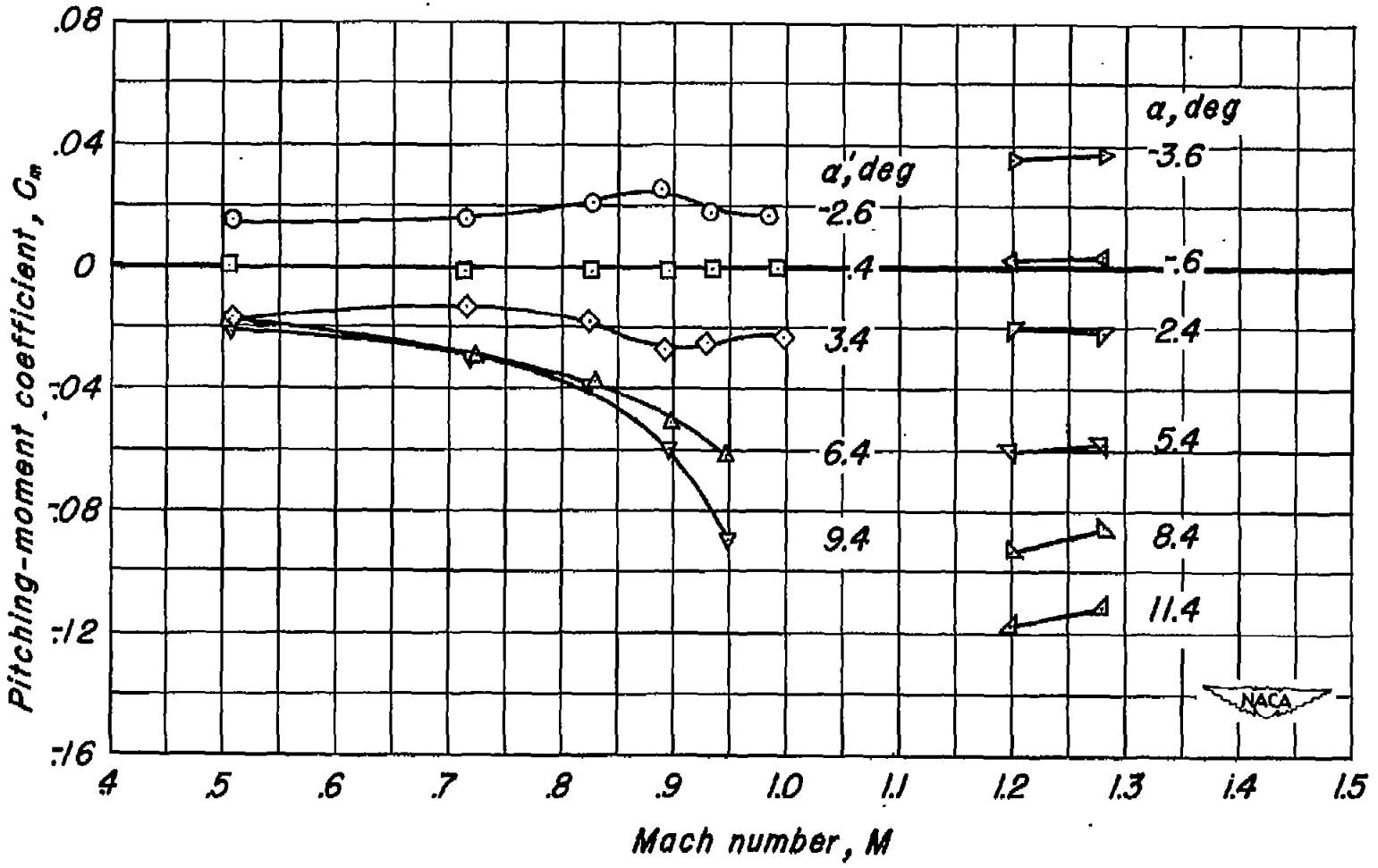

(b) Wing in presence of body.

Figure 9.- Concluded.

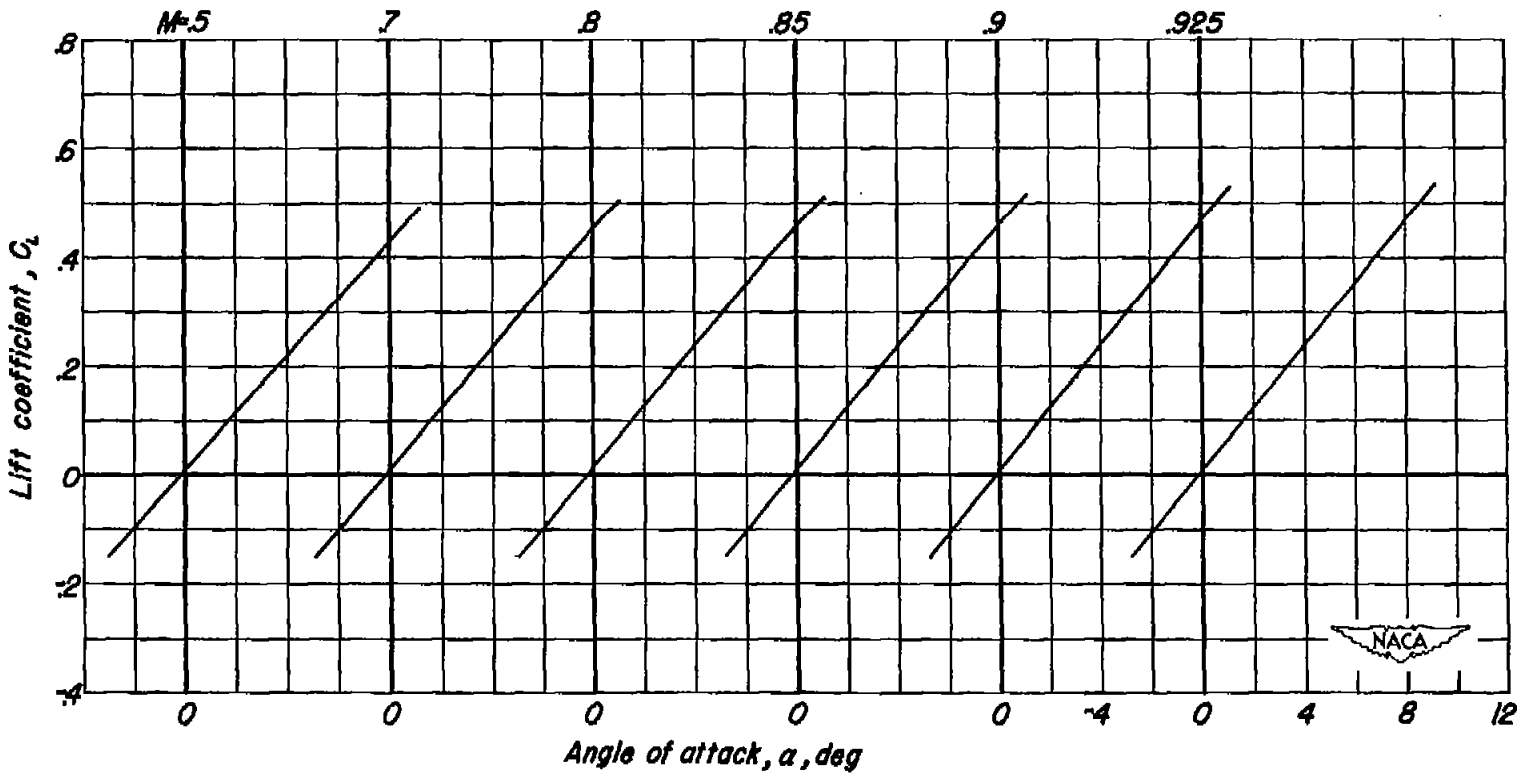

(a) Wing alone, gap unsealed; M, 0.5 to 0.925.

Figure 10.- Variation of lift coefficient with angle of attack for the wing alone and with the body, at several Mach numbers. Body attitude 0°.

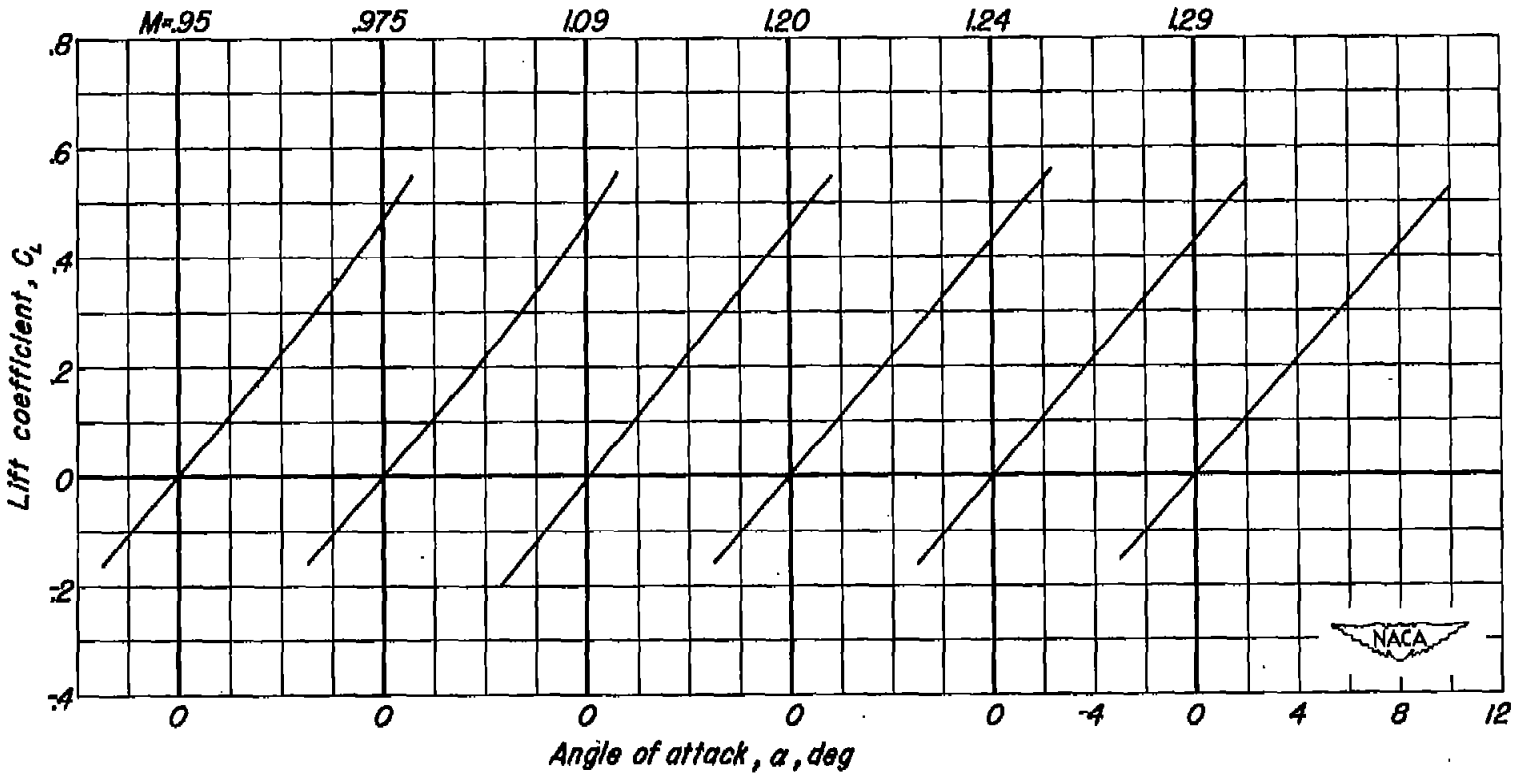

(b) Wing alone, gap unsealed; M, 0.95 to 1.29.

Figure 10.- Continued.

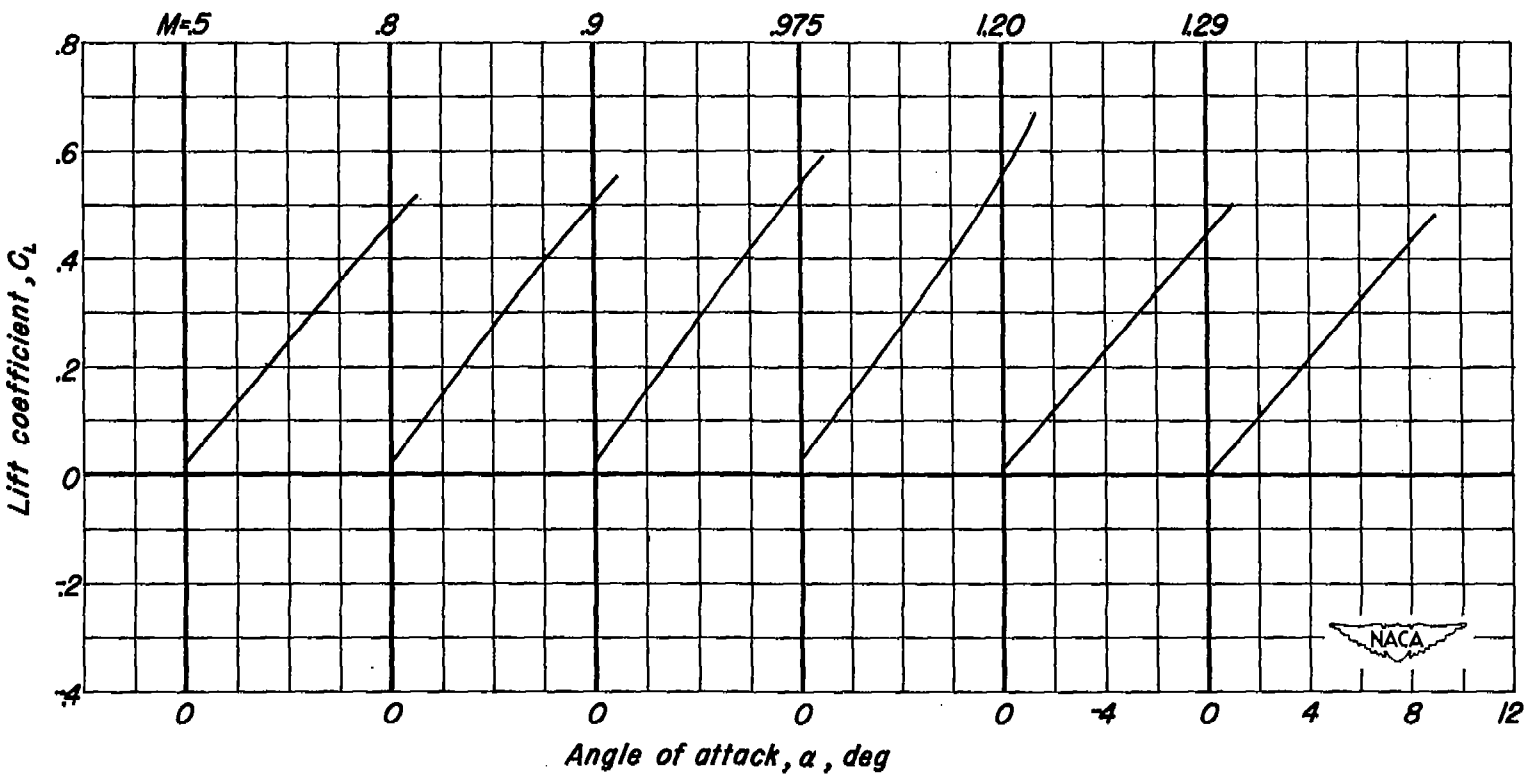

(c) Wing alone, gap sealed; M, 0.5 to 1.29.

Figure 10.- Continued.

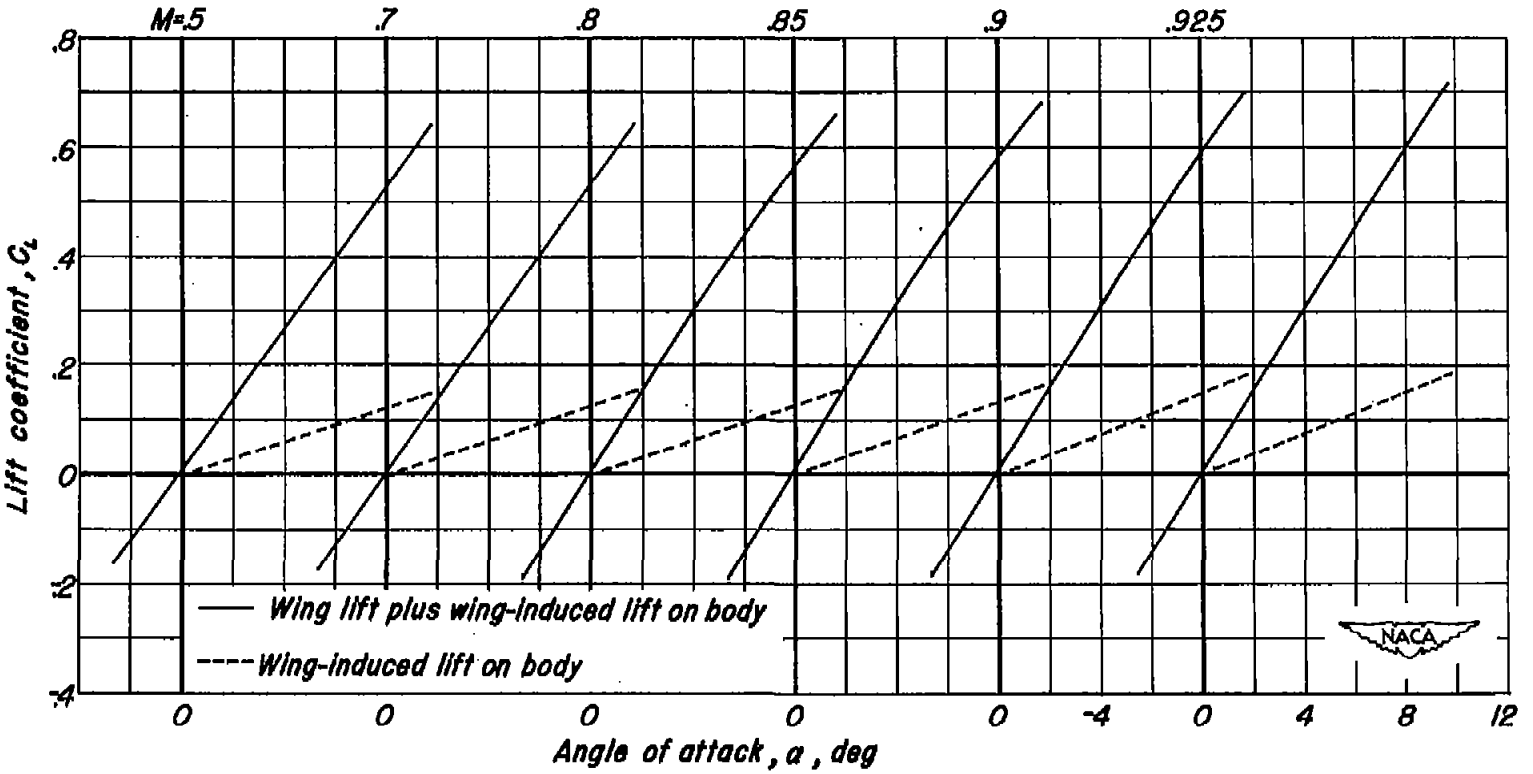

(d) Wing and body, gap unsealed; M, 0.5 to 0.925.

Figure 10.- Continued.

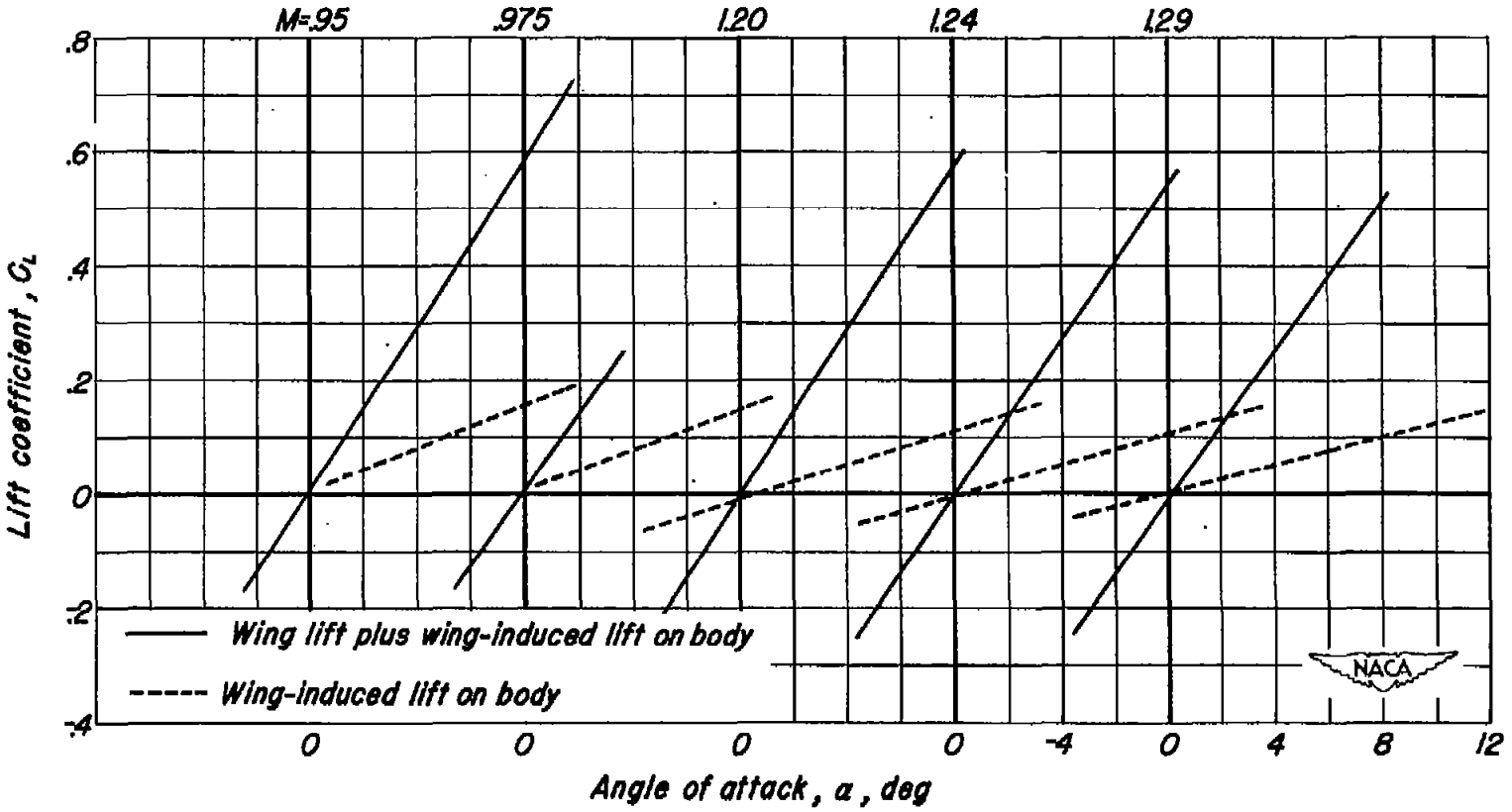

(e) Wing and body, gap unsealed; M, 0.95 to 1.29.

Figure 10.- Concluded.

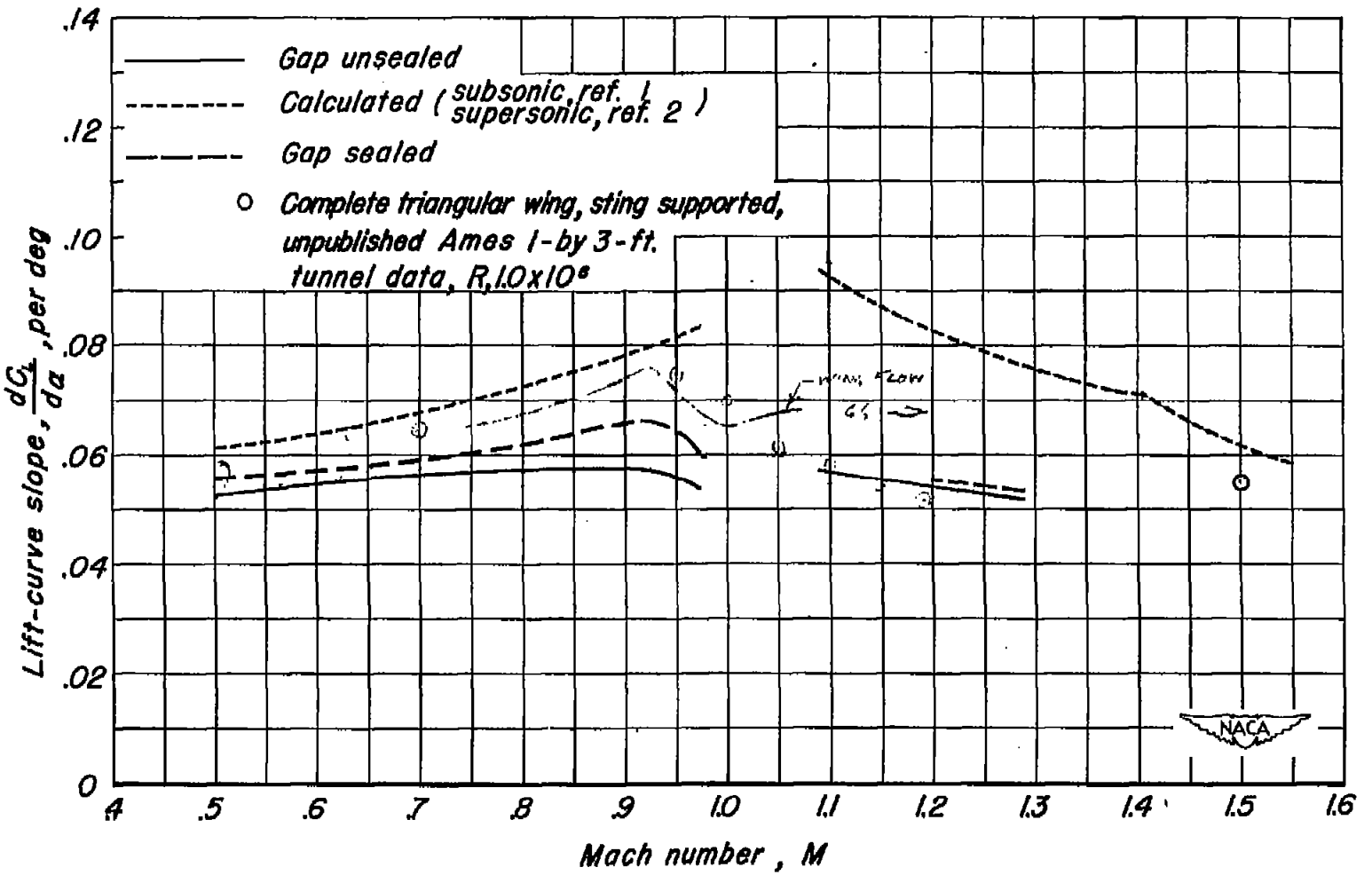

(a) Wing alone.

Figure 11.- Effect of Mach number on the lift-curve slope at low lift coefficients.

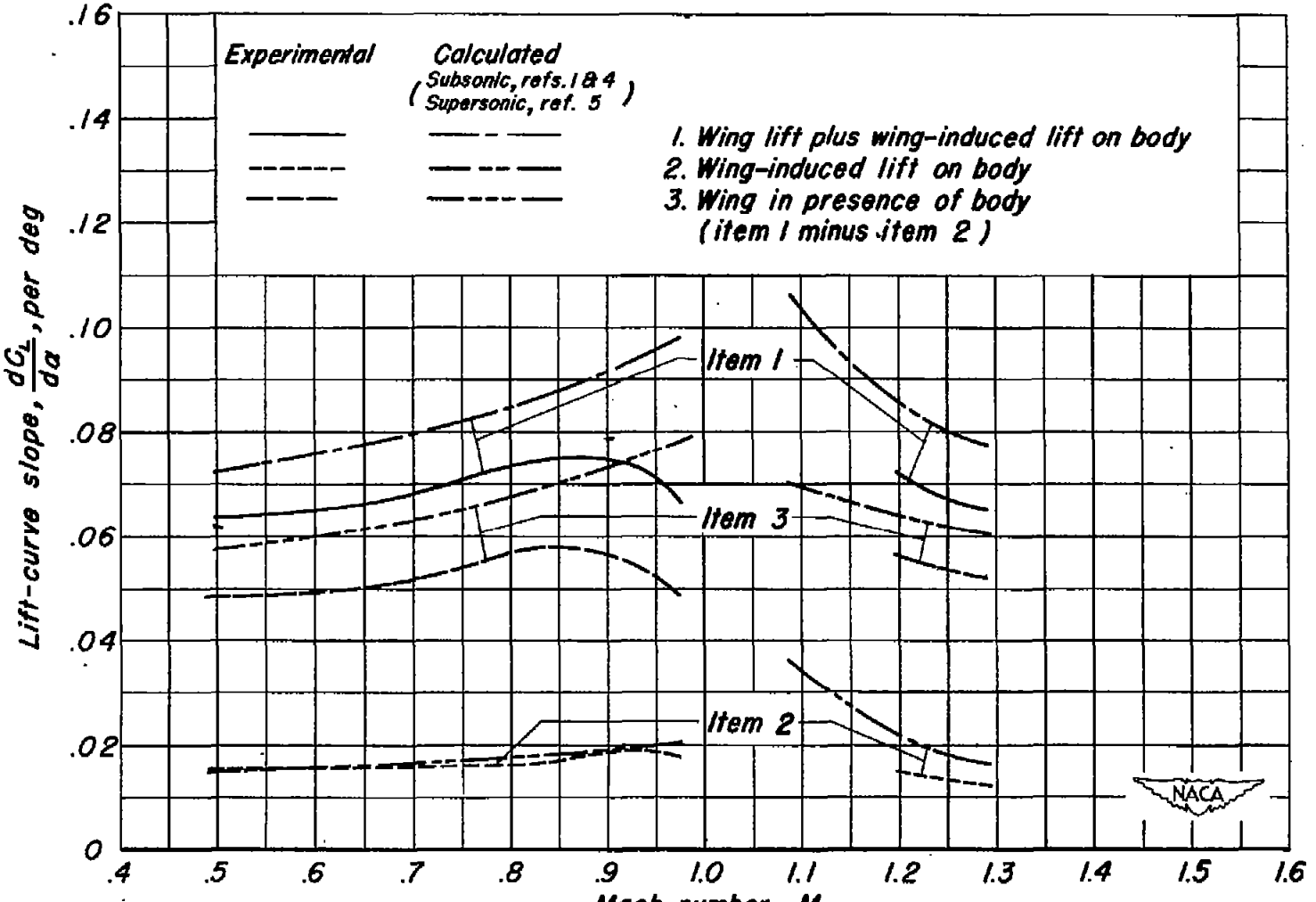

(b) Wing and body; body attitude 0°.

Figure 11.- Continued.

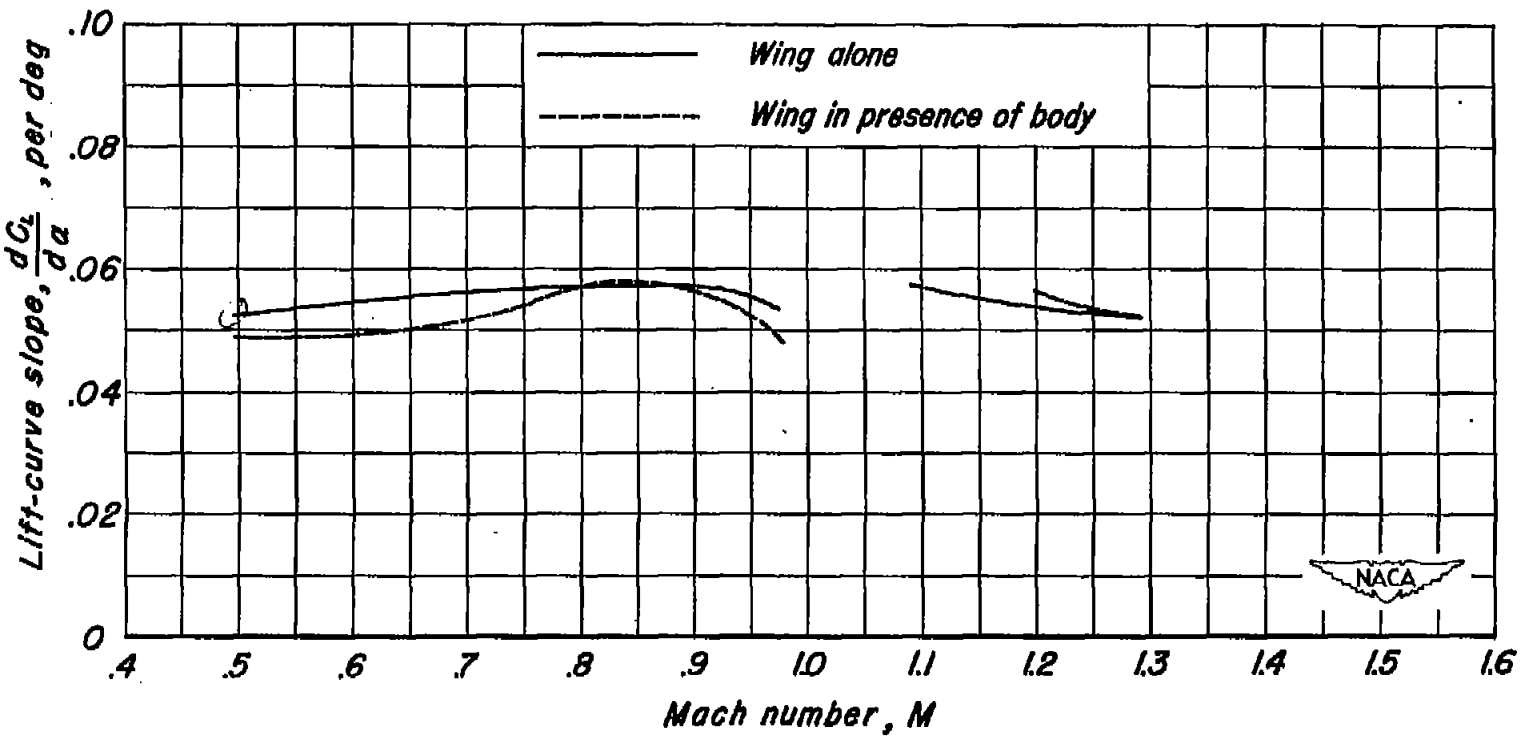

(c) Comparison of wing alone with wing in presence of body, gap unsealed.

Figure 11.- Concluded.

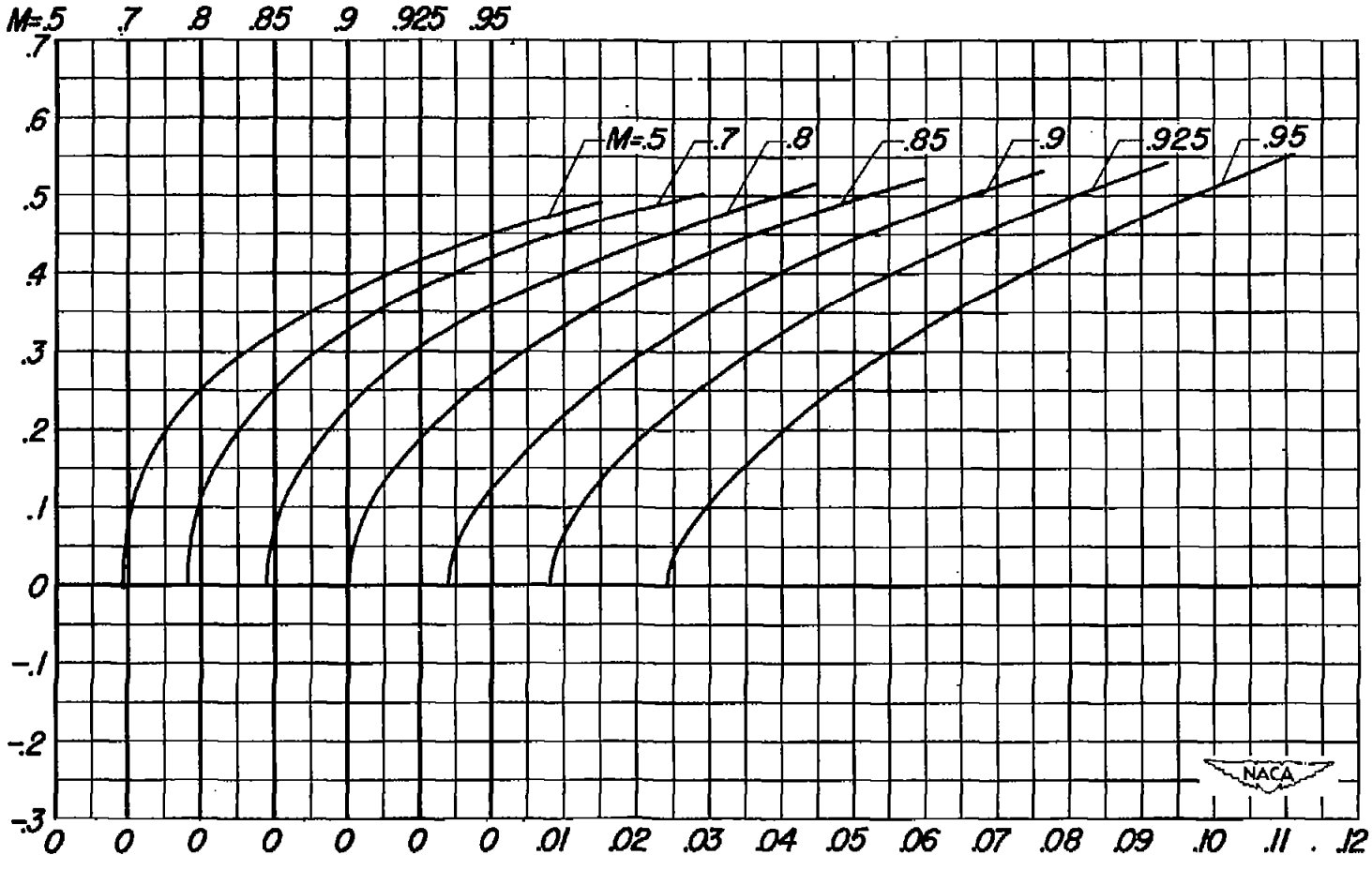

(a) M, 0.5 to 0.95.

Figure 12.- Variation of drag coefficient with lift coefficient for the wing alone at several Mach numbers, gap unsealed.

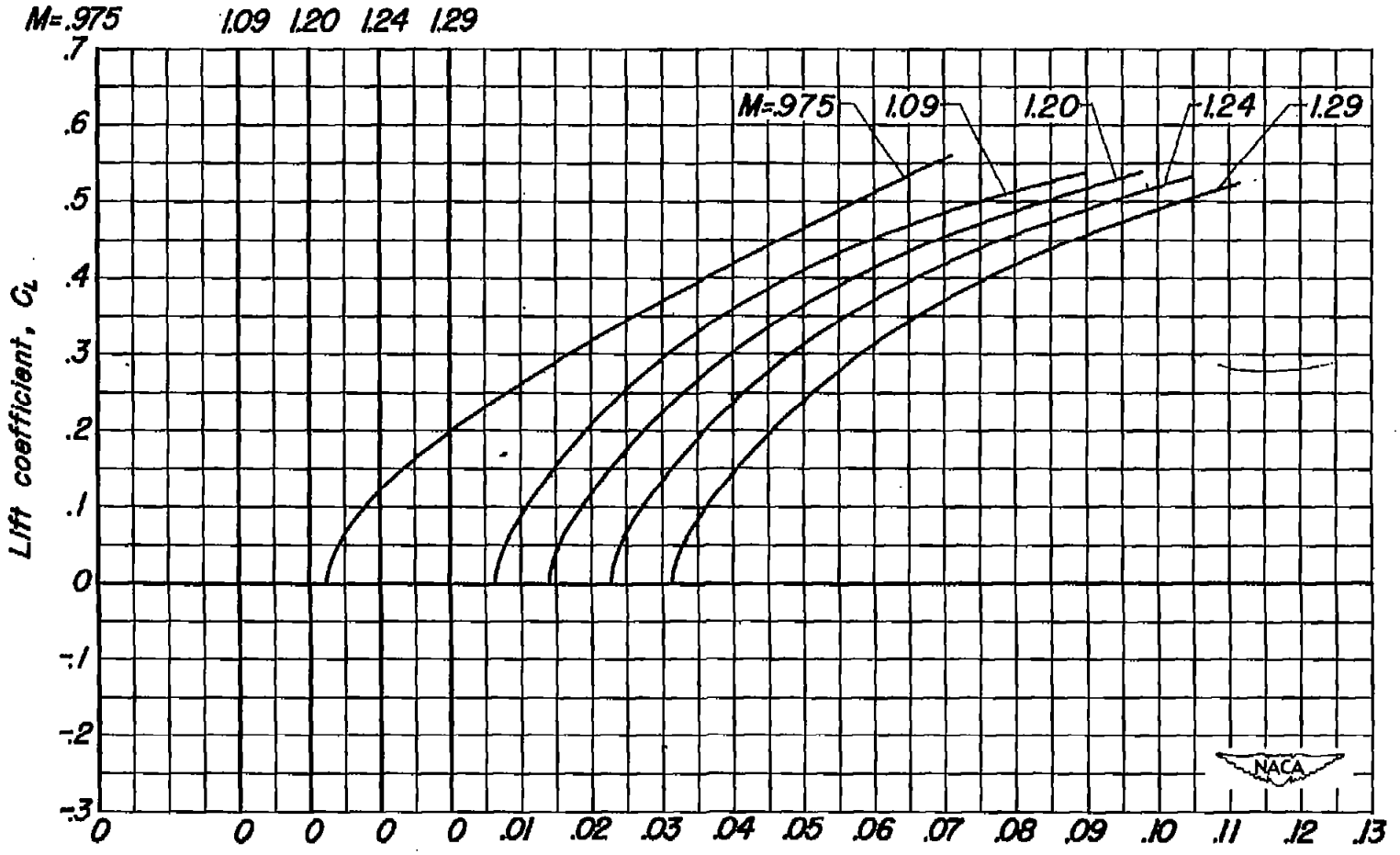

(b) M, 0.975 to 1.29.

Figure 12.- Concluded.

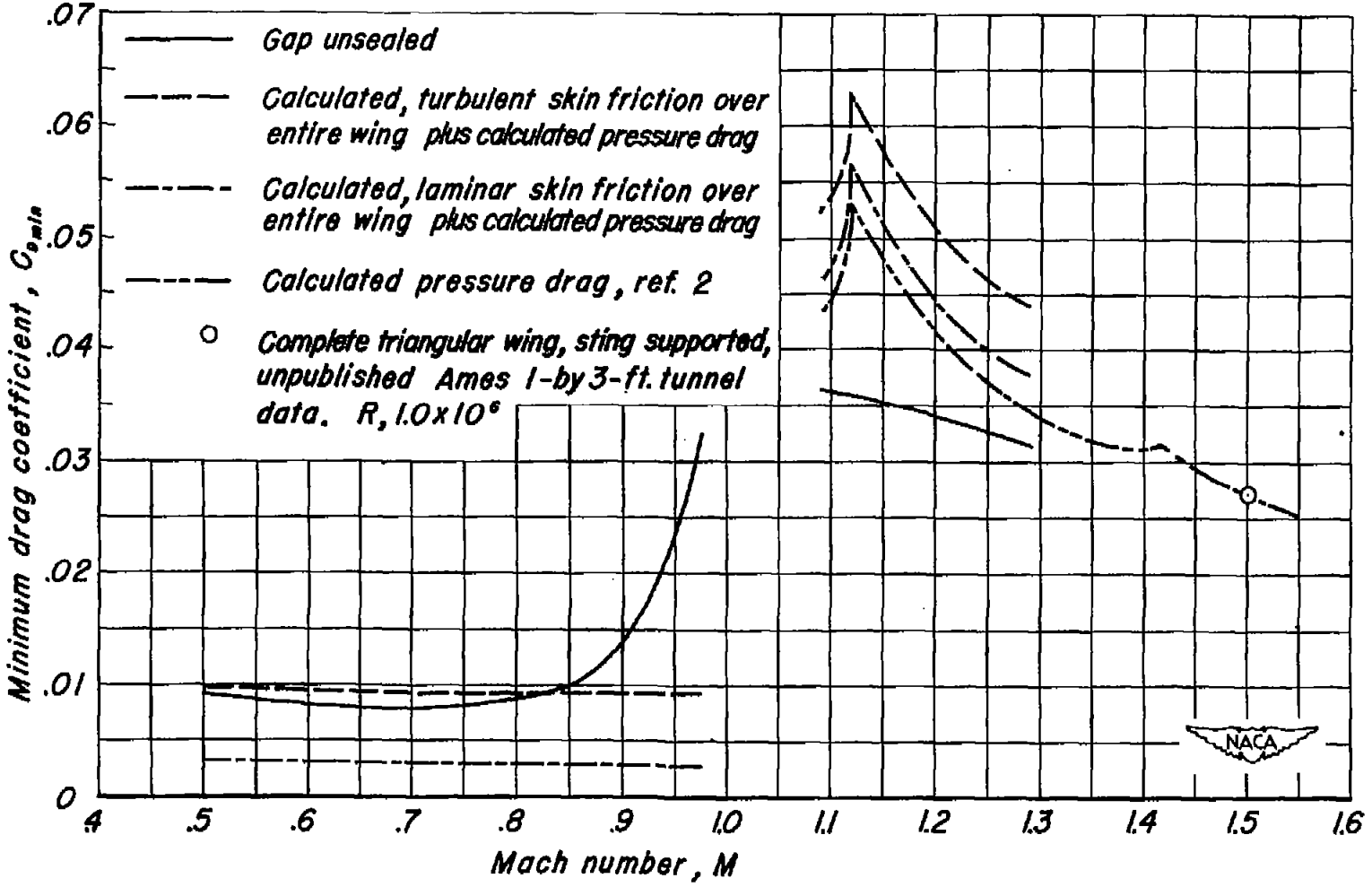

Figure 13.- Variation of the minimum drag coefficient with Mach number for the wing alone.

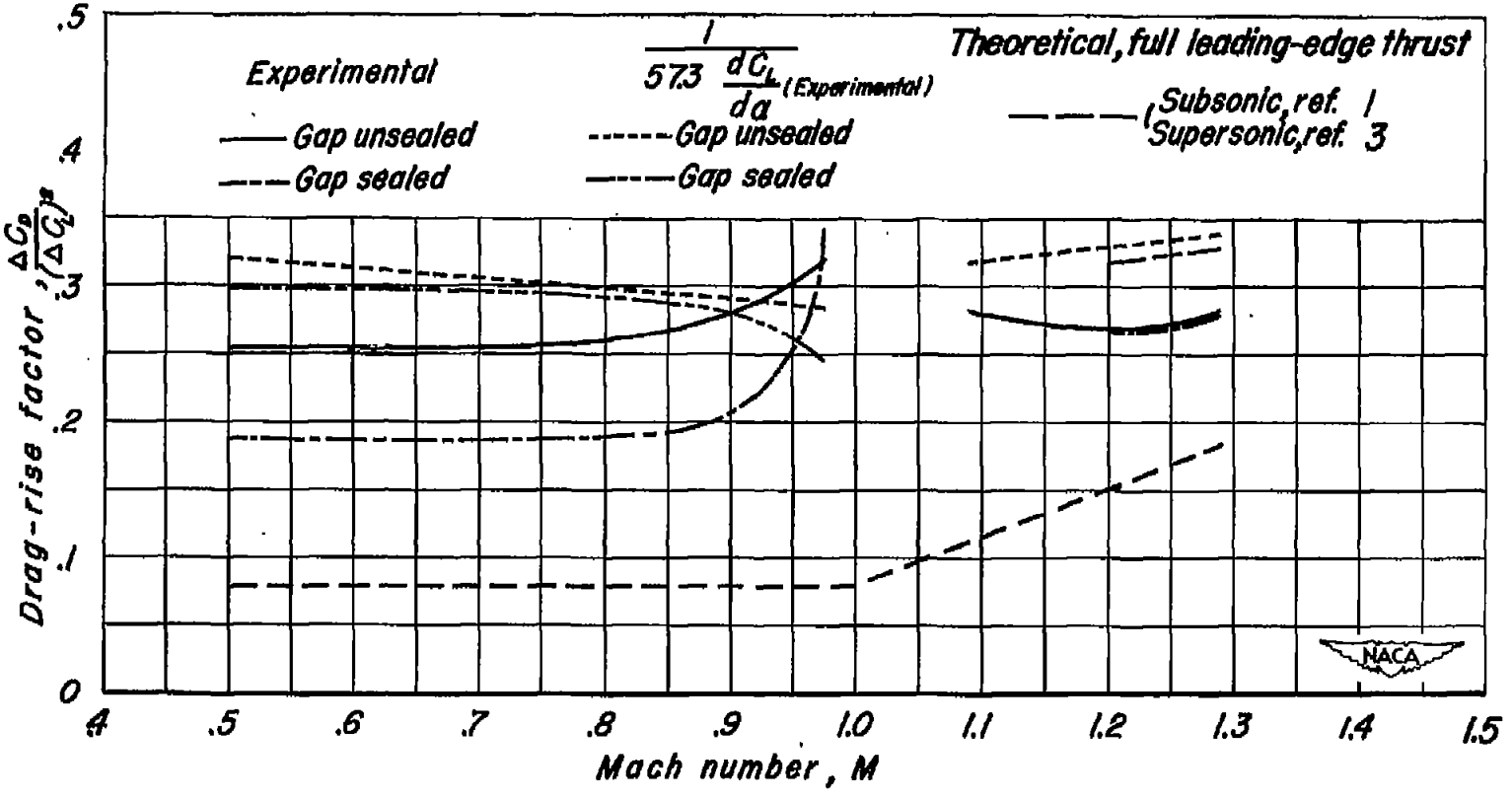

Figure 14.- Variation of the drag-rise factor with Mach number for the wing alone.

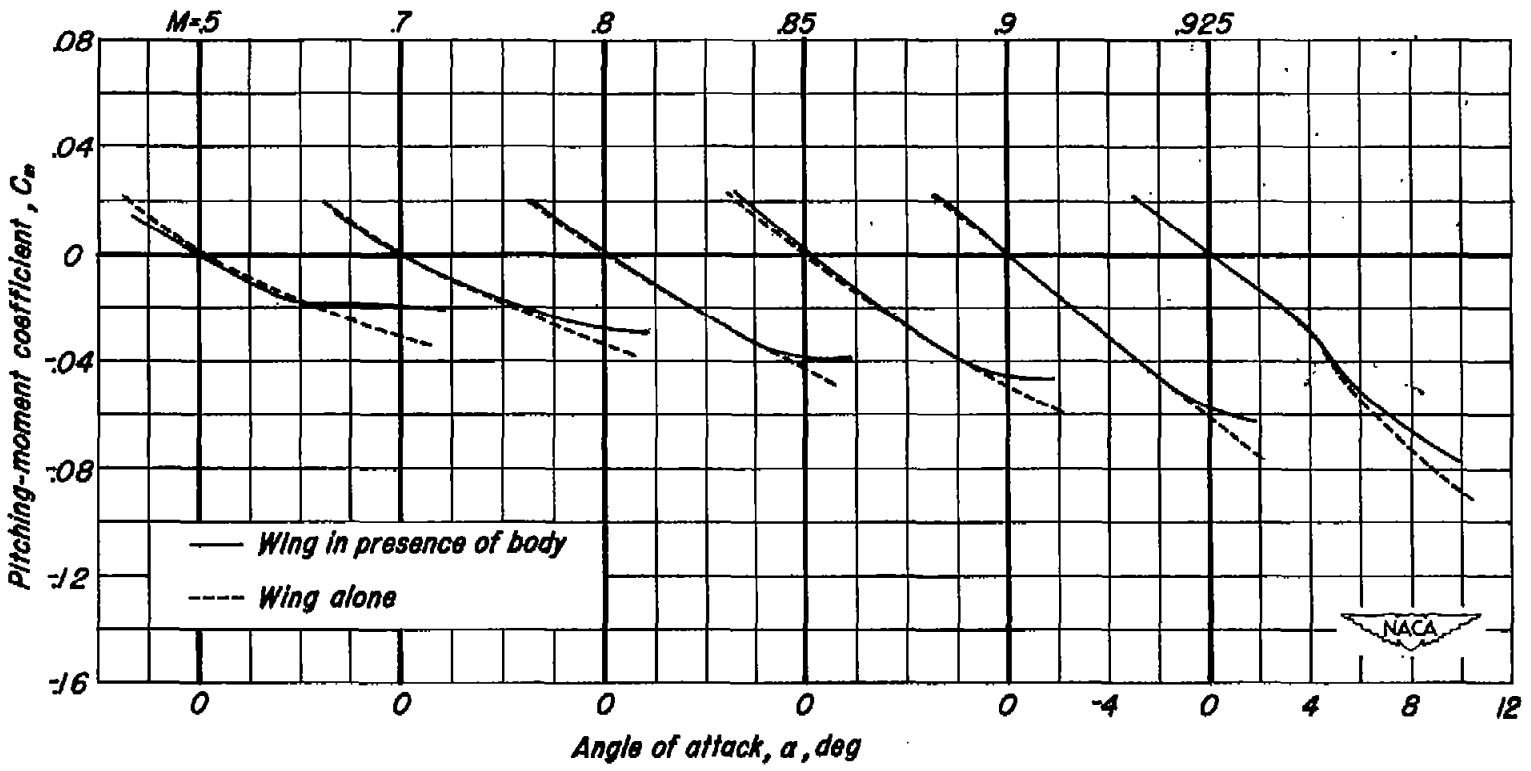

(a) M, 0.5 to 0.925.

Figure 15.- Comparison of the variations of pitching-moment coefficient with wing angle of attack for the wing both alone and in the presence of the body. Gap unsealed.

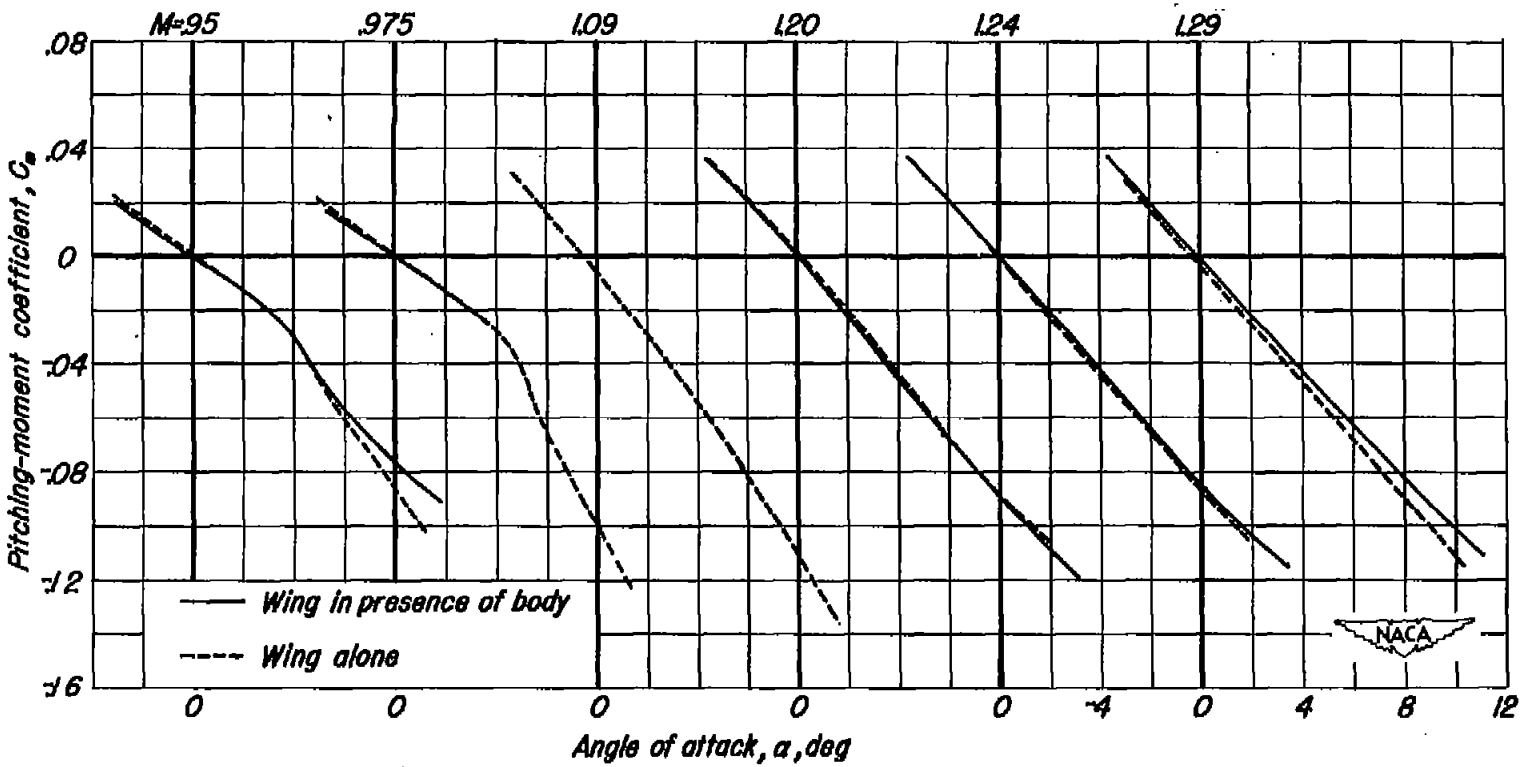

(b) M, 0.95 to 1.29.

Figure 15.- Concluded.

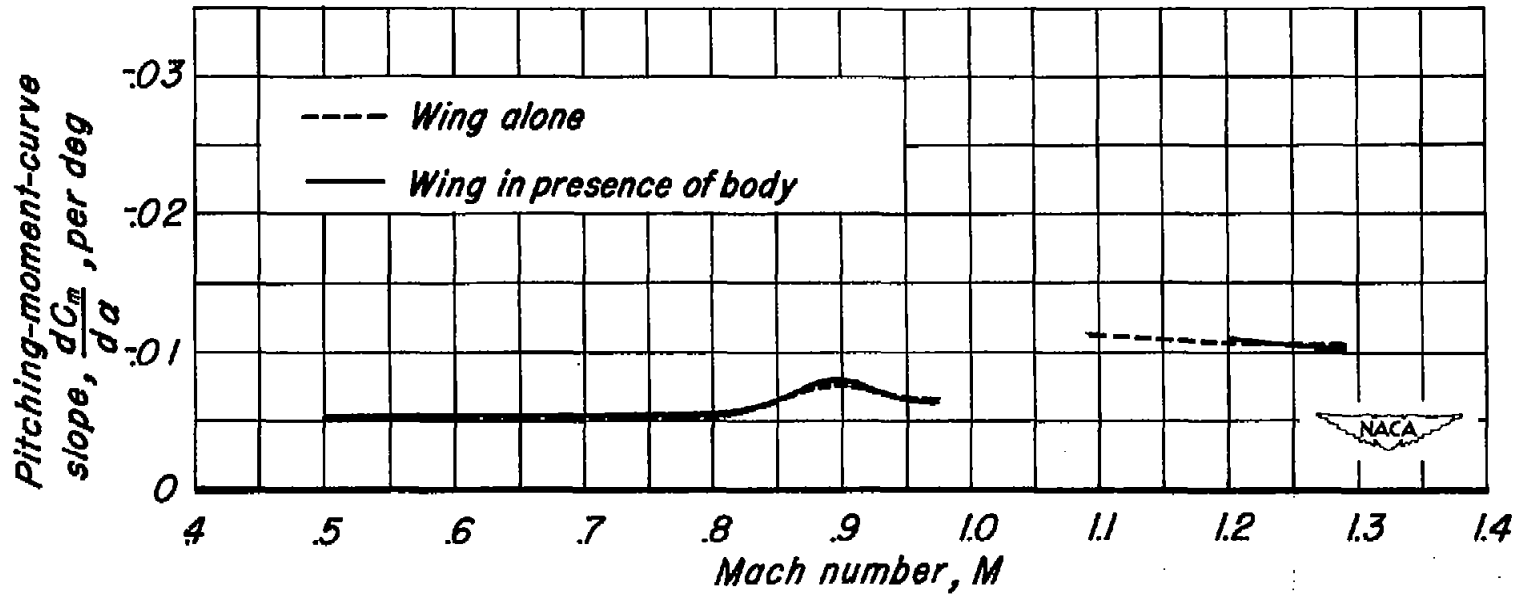

Figure 16.- Comparison of the variations with Mach number of the pitching-moment-curve slopes at zero angle of attack for the wing both alone and in the presence of the body. Gap unsealed.

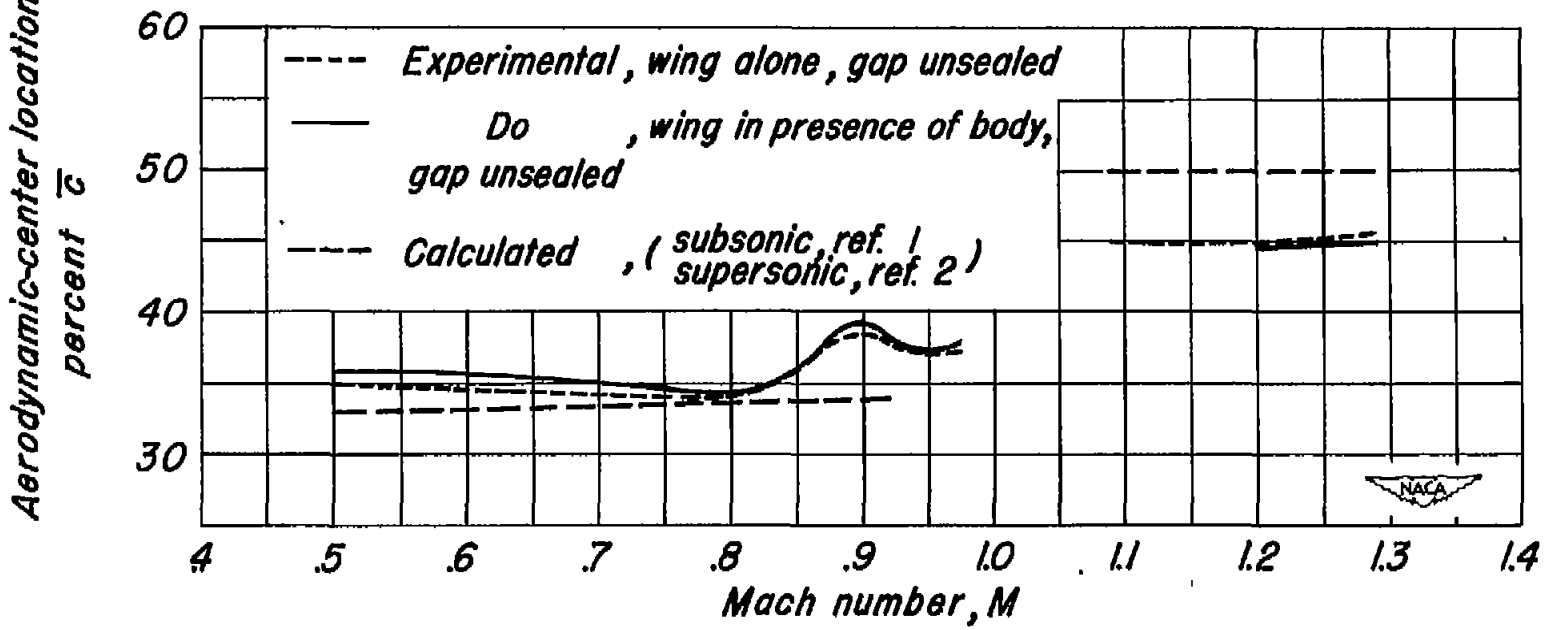

Figure 17.- Comparison of the variations with Mach number of the aerodynamic-center location at zero angle of attack for the wing both alone and in the presence of the body.